A

Project Report

On

Theoretical Analysis of Mixed Gas Adsorption Behaviour of (CH_4+CO_2) on Metal Organic Framework (MOF)

Submitted by

Saurabh Pandey

(Roll No: 109CH0086)

In partial fulfillment of the requirements for the degree in

Bachelor of Technology in Chemical Engineering

Under the guidance of

Dr. Pradip Chowdhury

Department of Chemical Engineering

National Institute of Technology Rourkela

May, 2013

CERTIFICATE

This is certified that the work contained in the thesis entitled ***"Theoretical Analysis of Mixed Gas Adsorption Behaviour of (CH_4+CO_2) on Metal Organic Framework (MOF),"*** *submitted by* ***Saurabh Pandey (109CH0086)****, has been carried out under my supervision and this work has not been submitted elsewhere for a degree.*

Date:

Place:

(Thesis Supervisor)

Dr. Pradip Chowdhury
Assistant Professor, Department of Chemical Engineering
NIT Rourkela

Acknowledgements

First and the foremost, I would like to offer my sincere gratitude to my thesis supervisor, **Dr. Pradip Chowdhury** for his immense interest and enthusiasm on the project. His technical prowess and vast knowledge on diverse fields left quite an impression on me. He was always accessible and worked for hours with me. Although the journey was beset with complexities but I always found his helping hand. He has been a constant source of inspiration for me.

I am also thankful to all faculties and support staff of Department of Chemical Engineering, National Institute of Technology Rourkela, for their constant help and extending the departmental facilities for carrying out my project work.

I would like to extend my sincere thanks to my friends and colleagues. Last but not the least, I wish to profoundly acknowledge my parents for their constant support.

_____

(Saurabh Pandey)

109CH0086

ABSTRACT

Separation of carbon dioxide from methane is an important issue in the processing of low-quality natural gases such as biogas, coal-seam, and landfill gases. Also, to encourage utilization of low-quality natural gases for energy and transport applications, the economics of CO_2 removal is the most critical step in the separation of CO_2/CH_4 mixture. To date, numerous approaches have been used for the bulk separation of CO_2 from CH_4. The conventional absorption/ stripping technology employed in the natural gas industry uses amines and/or glycol derivatives for the selective removal of CO_2, which is generally applicable to very large volumes of gas. Such processes are not only energy demanding but also, the volatile solvents involved might undergo degradation and loss during the operation, that results in negative environmental impact. In contrast, the adsorptive separation of CO_2 is commonly considered a more energy-efficient and economical alternative for smaller volume applications. Considerable attention has been given to the development of adsorption processes such as pressure swing adsorption (PSA), which is mainly based on differences in adsorption equilibrium and kinetics. Selection of a proper adsorbent with adequate selectivity, capacity, and diffusivity is an important step in designing the practical adsorption processes. Most reported studies of CO_2/CH_4 separation have focused on zeolites, functionalized mesoporous silica adsorbents, active carbons, and basic resin.

Recently, metal organic frameworks (MOFs) have been recognized as a new class of nanoporous materials that have many potential advantages over the traditional adsorbents. They are synthesized using organic ligands and metal clusters that self-assemble to form crystalline materials with well-defined structures, controlled pore size, high surface area, and desired chemical functionalities. These attractive properties make MOFs promising materials for gas separation and storage.

Any realistic process development requires estimation and/or prediction of mixed gas adsorption behavior. Invariably, any industrial process involves mixture of gases to be separated. The practical demonstration of such a process at laboratory scale is an extremely cumbersome exercise and there is a scarcity on mixed gas experimental data in literature and more specifically

on MOFs. It is pragmatic to gauge the efficiency of a particular adsorbent towards specific separation at the lab scale before being implemented at industrial level in a pressure swing adsorption (PSA) column.

This work is aimed at predicting the mixed gas adsorption behavior on MOFs. Pure gas adsorption data of CH_4 and CO_2 on various MOFs that has been reported over the years was taken from literature. Based on the Heat of Adsorption and the loading data collected CO_2 uptake capacity of all the MOFs has been found to be much more than that of CH_4. Plausible explanation has been given with data to support it.

The retrieved experimental data for Cr-BDC and Cu-BTC has been model fit using Dual Site Langmuir and Virial Langmuir respectively selected from a pool of standard isotherm models *viz*. Langmuir, Freundlich, Freundlich-Langmuir, and Virial models. The corresponding various model parameters have been found out and the binary or mixed gas behavior of (CO_2 + CH_4) mixture using IAST (Ideal Adsorbed Solution Theory) has been predicted. The separation factor has been found out and the possible use of Cu-BTC as a potential adsorbent in PSA column applications has been predicted.

CONTENTS

PAGE NO.

LIST OF TABLES

LIST OF FIGURES

LIST OF FIGURES

LIST OF FIGURES

LIST OF SYMBOLS

a	Specific area of adsorbent per mole of adsorbate, m^2 mol^{-1}
b	Second virial coefficient in adsorbed phase, $mmol^{-1}$ g
b_i	Affinity Parameters
b_i^0	Affinity at reference at T_o
c	Third virial coefficient in adsorbed phase, $mmol^{-2}$ g^2
f	Fugacity, bar
Δh_{ads}	Enthalpy of adsorption, kJ mol^{-1}
$\Delta h_{ads,0}$	Enthalpy of adsorption at zero loading, kJ mol^{-1}
K	constants for a given adsorbate and adsorbent at T
n	constants for a given adsorbate and adsorbent at a T
N	Amount adsorbed, mmol g^{-1}
N_i^{max}	saturation capacity
P	Pressure, bar
R	Universal gas constant, 8.314 J mol^{-1} K^{-1}
T	Temperature, K
T_o	reference temperature
x_i	Adsorbed phase mole fraction of species i
y_i	mole fraction of given gas i in the mixture
Z	Compressibility factor for the adsorbed phase

GREEK LETTERS

θ	Fractional coverage of the surface
α	Langmuir constant
ρ^{gas}	Density of gas
β	Henry constant, mmol g^{-1} bar^{-1}
ψ	Spreading Pressure
$\hat{\phi}_i^{gas}$	Fugacity coefficient of bulk gas
γ_i	Activity coefficient in adsorbed phase

CHAPTER 1

INTRODUCTION

This chapter highlights the basics on adsorption science and technology. It focuses on novel adsorbent materials called metal organic frameworks (or, MOFs). The background of the present thesis work is aptly explained. The objectives are also properly highlighted.

1.1 Prelude

Adsorption is the selective binding of a substance by another solid substance [Barrer, 1978]. In simpler words, it is the sticking of gaseous or liquid molecules (adsorbents) onto the surface of a solid material (adsorbate). The opposite of this i.e. the release of these adsorbed molecules from the solid surface is called as desorption. Unlike absorption, adsorption is a surface phenomenon that in principle occurs at any pressure and temperature. Based upon the strength or interaction energy, by which the adsorbed molecules are bound to the sorbent's surface, adsorption can classified as physisorption, physico-chemical adsorption and chemisorptions.

- *Physisorption* or physical adsorption is the type of adsorption in which the adsorbate molecules adhere to the surface through Van der Waals (weak intermolecular) and/or dispersion forces that are caused due to induced dipole-dipole interactions, which are also responsible for the non-ideal behaviour of real gases. They can also be desorbed reversibly by lowering the sorptive gas pressure gas pressure or increasing the temperature.
- *Physico-chemical adsorptions* are associated with weak interactions among the sorbent atoms and the admolecules. However, dissociation or fairly strong association may occur because of the catalytic properties of the sorbent surface.
- *Chemisorption* is the type of adsorption in which a molecule adheres to a surface by forming a chemical bond, as opposed to the weaker Van der Waals forces which cause physisorption. Admolecules cannot be desorbed reversibly from the sorbent, but only irreversibly by which the sorbent material is changed.

Adsorption is usually described through isotherms, which basically are functions which connect the amount of adsorbate on the adsorbent, with its pressure (if gas) or concentration (if liquid). One can find in literature many such models describing process of adsorption, namely Langmuir isotherm, Freundlich isotherm, Virial Isotherm, Kisliusk Isotherm, BET isotherm, Toth etc.

One of the most important uses of adsorption is in the gas separation processes. Separation can be defined as a process that separates a mixture of substances into two or more product that differs from each other in composition. The process is rather difficult to achieve because it is opposite of mixing, a process supported by the second law of thermodynamics. Separation steps in chemical and petrochemical industry account for the major production cost. Gas Separation can itself be based on one or more of the following effects:

a) *Mixture adsorption equilibria*: One component gets adsorbed much more than the others
b) *Adsorption kinetic effects*: One component diffuses through the adsorbent much faster than the other
c) *Molecular sieve or steric effects*: bulky molecules prevent fluid molecules from entering a pore (system)
d) *Quantum sieve effects in so-called nanopores:* This effect is of importance for separating hydrogen or deuterium from other gases

1.2 Novel Adsorbents

New materials usher new technologies. Synthesizing novel materials is always reflected as a corner stone in technological developments. Until recently, zeolites and activated carbons are thought to be the indispensable in adsorption based unit operations. But as the need grows for more efficient, economical and highly specific functions, conventional adsorbents were found ill equipped to handle such problems. Although, improved synthesis and different post-treatment procedures of zeolites and activated carbon resulted into some of their derivatives but the need of the hour was to design and synthesize materials that could be more effective.

In the quest for designing novel adsorbents, attention has been paid to develop hybrid structures involving both inorganic and organic components by employing novel synthetic routes. The general concept was to take advantage of both the metal coordination and functionalities of the organic components. The concept of reticular synthesis which can be described as the process of assembling judiciously designed rigid molecular building blocks into predetermined ordered structures or networks, held together by strong bonding is found to be the key to the true design of novel solid-state materials. Researchers have envisioned that to fully realize the benefits of designing crystalline solid state frameworks the structural integrity and rigidity of the molecular building blocks must remain unaltered throughout the construction process: key feature of reticular synthesis [9]. The said mechanism plays a pivotal role in producing robust porous materials by connecting rigid rod-like organic moieties with inflexible inorganic clusters acting as joints. The length and functionalities of the organic units determine the size and chemical environment of the resulting void spaces. Accordingly, the concept of "tailor-made" materials finally realized. Appropriate selection of starting materials can give rise to myriad of different structures. Within a short period of time a large variety of extended structures have been successfully prepared and the collection of compounds has been given various names e.g. "coordination polymers", "hybrid organic-inorganic materials", "organic zeolite analogues" or "metal organic frameworks". Although each terminology signifies certain aspects of the materials it encompasses but for a solid to be truly called a "Metal Organic Framework" or MOF, it must possess robustness implying strong bonding, assembling units are available for modification by organic synthesis and geometrically a well-defined structure.

1.3 Background of present research work

Some conventional well-known adsorbents include: silica gel, activated alumina, activated carbon, carbon molecular sieves and zeolites. Each of these adsorbents has certain specific features that have been exploited over the years in various industrially challenging applications ranging from adsorptive gas separation/purification, ion-exchange and catalysis. In this present context, the term "Novel" signifies a new class of hybrid adsorbents popularly known as "metal organic frameworks" or MOFs

In recent years, metal organic frameworks (MOFs), i.e. porous three-dimensional coordination polymers, become more and more interesting since their matrix and pore characteristics (high specific surface area and microporosity, definite pore size distribution, structural regularity, flexibility, etc.) promise applications in gas storage, catalysis, ion exchange, separation, polymerization, etc. [46]. In this way, the number of microporous solids such as zeolites and activated carbons applicable in chemical industry is extended.

The first structures of coordination polymers have been already reported in the early 1960s [47–49], but with the synthesis of HKUST- 1 ($Cu_3(btc)_2$, btc = 1,3,5-benzene tricarboxylate) and MOF-5 in 1999 [61,62], MOF materials became really popular. HKUST-1 and the recently presented DUT-6 possess impressive high specific surface areas [61, 66, 67].

With regard to the search for applications of MOFs it is advantageous that a vast variety of metal ions, i.e. inorganic nodal points [68], and organic linkers can be used to synthesize different structures of coordination polymers.

1.3.1 Selection of MOFs

A careful review of the literature reveals more than 2,000 different MOF structures being synthesized and characterized. Although the number speaks volumes about their variation in structural configuration but not all are stable. Thermal and chemical stability, along with high surface area is what researchers look for in a good adsorbent to be effective at the industrial level. Cu-BTC (or HKUST-1), Cr-BDC (or MIL-101) and Zn-BDC (or, MOF-5) frameworks possess all the desirable qualities that set them apart from others. Not only they have very high specific surface areas but also show better stability. Some of their characteristic features include:

- High specific surface area (~1000 to 5000 m2/g), large pore volume (~0.7-2.5 cc/g) and light weight or low packing density
- Low to moderate heat of adsorption (15-20 kJ/mol)
- Good thermal and chemical stability

1.3.2 Selection Of Gases

Carbon dioxide and methane separation is an important issue in the processing of low-quality natural gases such as biogas, coal-seam, and landfill gases. The presence of CO_2 with CH_4 not only reduces the energy content of natural gas but also causes pipeline corrosion [31, 53]. CO_2 must be removed to concentration below 2–3% in the pipeline-grade methane before being used for low-temperature processing [54]. Biogas is also a very important source of renewable methane that is produced by the decomposition of organic matter under anaerobic conditions. CO_2 happens to be the major non combustible component (25–45%) that must be separated from the biogas [55]. Coal seam gas mainly contains CH_4 with higher hydrocarbons as well as contaminants such as CO_2 and N_2 [56]. Landfill gas consists of primarily CH_4 (50–65%) and CO_2 (35–50%) as well as a small amount of N_2 and sulphur compounds [58]. To further encourage utilization of low-quality natural gases in energy and transport applications, the economics of CO_2 removal is identified as the most critical step in the separation of CO_2/CH_4 mixture. Table 1.1 lists several CO_2 and CH_4 emissions as reported by Ministry of Environment and Forests, Government of India, 2012 to the United Nations Framework Convention on Climate Change.

Table 1.1: India's national greenhouse gas inventories of anthropogenic emissions by sources of greenhouse gases for the year 2000.

Greenhouse gas source and sink categories	CO_2 (emissions)	CO_2 eq. Emissions*
Total (Net) National Emission (Giga gram per year)	**1,024,772.84**	**1,301,209.39**
1. All Energy	**952,212.06**	**1,027,015.54**
Fuel combustion		
Energy and transformation industries	541,191.33	543,749.85
Industry	228,246.91	229,079.90
Transport	95,976.83	9,8104.12
All other sectors	86,797.00	127,686.10
Fugitive Fuel Emission		
Oil and natural gas system		16,096.83
Coal mining		12,298.74
2. Industrial Processes	**72,560.78**	**88,608.07**
3. Agriculture		**355,600.19**
Enteric Fermentation		211,429.43
Manure Management		5,087.77
Rice Cultivation		74,360.56
Agricultural crop residue		6,911.96
Emission from Soils		57,810.47
4. Land use, Land-use change and Forestry*		**(222,567.43)**
Changes in Forest and other woody biomass stock		(203,704.42)
Forest and Grassland Conversion		(18,788.08)
Settlements		(75.55)
5. Other Sources as appropriate and to the extent possible		**52,552.29**
5a.Waste		
5b. Emissions from Bunker fuels #	**3,467.12**	**3,498.86**
5c. CO_2 emissions from biomass #	**376,005.00**	**376,005.00**

To date, numerous approaches for the bulk separation of CO_2 from CH_4 have been used. The conventional absorption/stripping technology employed in the natural gas industry uses amines [59] and/or glycol derivatives [53] for the selective removal of CO_2, which is applicable generally to very large volumes of gas. Such processes are energy demanding due to the relatively high regeneration temperatures and the need for recycling a large amount of water. Additionally, the volatile solvents might undergo degradation and thus loss during the operation that results in negative environmental impact. In contrast, the adsorptive separation of CO_2 has been commonly considered as a more energy-efficient and economical alternative for smaller volume applications [60].

1.4 Research Objectives

I. *To collect pure gas isotherm data of CH_4 and CO_2 on various contemporary MOFs.* The experimental gas adsorption data tends to vary lab to lab. As a result, crucial properties, such as pore volume and surface area of the MOF that is used for each of the two gases, may different slightly. Hence, in order to maintain uniformity and avoid any discrepancies, the pure gas isotherm data of the two gases on a particular MOF, is to be considered if only it's from the same lab.

II. To screen the above data and find the most suitable MOF adsorbent based on :

   i. *Their individual loading capacity.* The cases of MOFs for which the individual loadings are more are to be selected. This is due to the fact that MOFs with higher capacity indicate greater adsorption, and are thus profitable preferred in any industry.

   ii. *Moderate Heat of adsorption.* The heat of adsorption indicates how strongly molecules of the gas are adsorbed onto the adsorbent. If the bond is weak, adsorption isn't proper and the gas separation capacity of the process as a whole is reduced. However, if the molecules are adsorbed too strongly, desorption during regeneration cycle gets difficult.

iii. *Regeneration Potential after multiple cycles of operation.* After several cycles of adsorption and desorption, MOFs tend to wear out, thus decreasing their adsorbing capacity. This is due to several factors, such as modified surface properties, caused by the heat evolved during adsorption. A MOF with higher Regeneration Potential is always preferred.

iv. *Availability of suitable/concrete data at various optimum conditions*. To improve generality of the results obtained, the case for which the data is available at more than just one Temperature and Pressure is to be considered.

III. *Fitting of experimental data obtained as above with suitable Thermodynamic model and existing model parameters*. The several Adsorption Isotherm models discussed earlier are to be used and factors such as n, b, c, regression coefficient, adsorption coefficient etc. are to be found out.

IV. To Predict binary or mixed gas behavior of (CO_2 + CH_4) mixture using thermodynamic models with special focus on IAST (Ideal Adsorbed Solution Theory).

V. Prediction of separation factor and validation with experimental data (retrieved from literature) and lab results for examining its suitability in PSA applications.

CHAPTER 2

LITERATURE REVIEW

In this chapter a brief review on metal organic frameworks (MOFs) is given. A general overview on adsorption of H_2, CO and CO_2 on various conventional and novel adsorbent materials is also represented in tabular form. The intention is to highlight the frequency of work in this field and gradual improvement in experimental data on adsorption of these gases on MOFs and other conventionally known adsorbents *viz.* zeolites, activated carbon etc.

2.1 Metal Organic Frameworks (MOFs)

2.1.1 Brief Review

"Metal Organic Frameworks" or MOFs represent a class of novel materials that has caught the attention of researchers owing to their great diversity in structures resulting from co-ordination between inorganic metal atoms/ions and organic ligands as linkers. Proper selection of metal atoms/ions and organic linkers leads to innumerable possibilities in the co-ordination geometry with wide variation in structural architecture. A few very attractive motifs include honeycomb, brickwall, bilayer, ladder, herringbone, diamondoid, rectangular grid, and octahedral geometries. Metal Organic Frameworks (MOFs) which forms as a result of combination of an inorganic metal atom/ion as a node with an organic ligand as a linker can be classified to be a relatively new group of materials. Ever since initial reports on its synthesis, there has been a spurt in research activities owing to some of their characteristic features. The most important features include: extremely high specific surface area (*ca.* 800-5000 m^2 g^{-1}) and large pore volume (*ca.* 0.8-2.5 cc g^{-1}), uniform pore size distribution and tunable or tailor-made pores.

2.1.2 MOF Architecture

The key to successfully designing metal organic frameworks lies in the use of linkers meant to achieve desired network topologies by connecting transition-metal centers or polynuclear clusters serving as nodes of the network. Myriad of different possibilities are there depending on

our choice of metal atoms/ions and organic linkers. Flexibility or the rigidity of the frameworks is greatly affected by the choice of organic linker in the structure. To illustrate the complete behavior let us consider the following example [9]

In Figure 2.1 (**A**), we have the assembly of a tetrahedrally coordinated metal center and a linear organic linker like 4, 4´-bipyridine. It results in a structure with an expanded diamond topology. Each bond of the diamond network is replaced by a sequence of bonds that expands the networks and yields void space proportional to the length of the linker. In Figure 2.1 (**B**) the organic linker is 1, 4-benzene dicarboxylate. It allows for the formation of an aggregate of metal ions into M-O-C clusters that generally referred as secondary building units (SBUs) which finally extends into a cube.

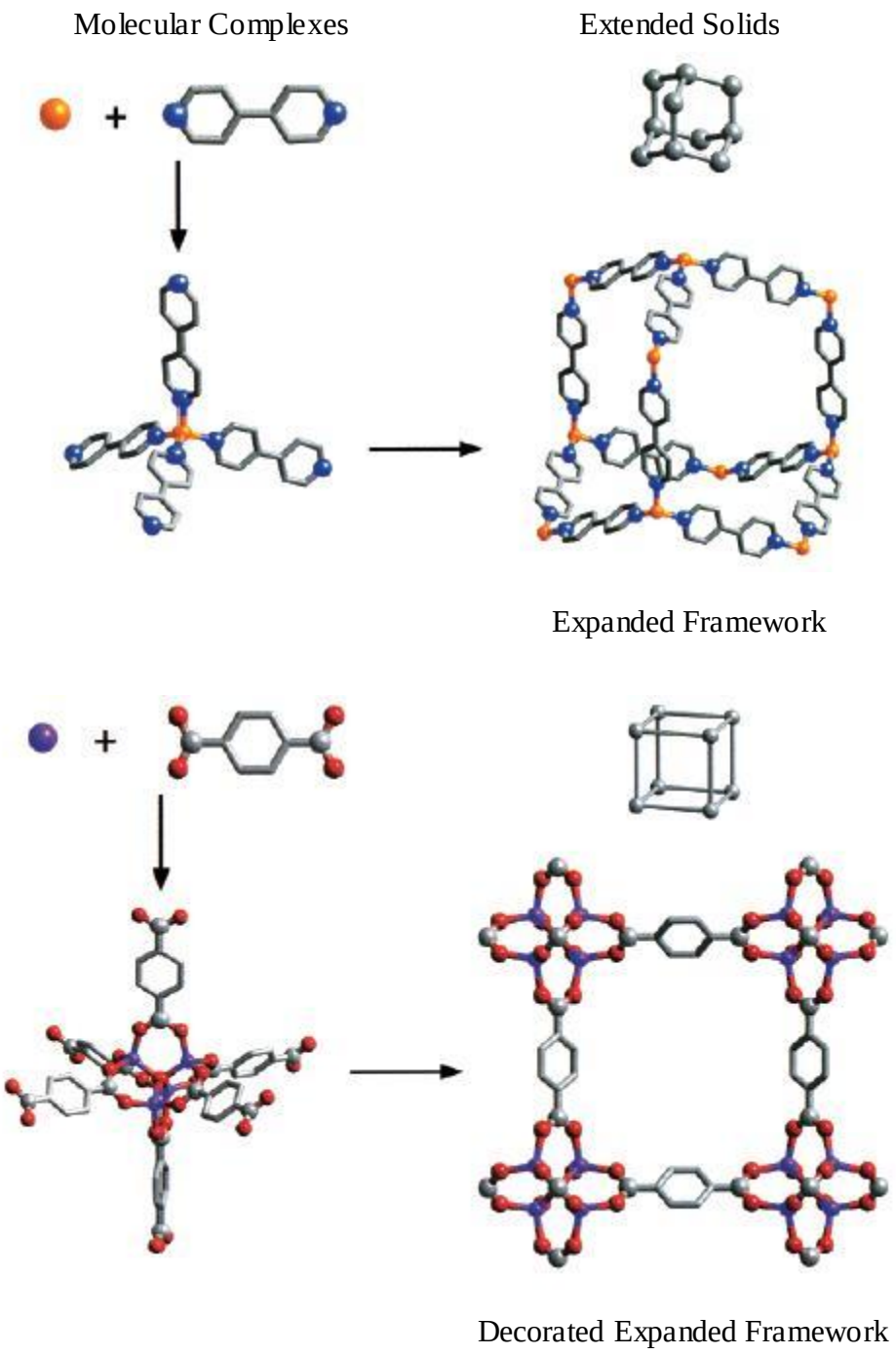

Figure 2.1: Assembly of Metal Organic Frameworks. (**A**) Flexible metal-bipyridine structures with expanded diamond topology (Metal-orange, Carbon-gray, Nitrogen-blue) (**B**) Rigid metal-carboxylate clusters expanding into a cube (Metal-purple, Carbon-gray, Oxygen-red). For the sake of clarity all hydrogen atoms are not shown [9].

2.1.3 Salient Features of MOFs

Some of the characteristic features of MOFs include:

(a) High surface area (*ca*. 800-5000 $m^2 g^{-1}$) and pore volume (*ca*. 0.5-2.5 ml g^{-1})

(b) Highly crystalline and can be synthesized in pure form with less crystal imperfections

(c) Uniform pore size distribution akin to zeolites and hence good molecular sieving properties

(d) Low to moderate heat of adsorption and hence can act as a good gas storage medium

(e) Low bulk packing density i.e. lighter in weight

Although MOFs have shown some remarkable features but still there are certain unresolved issues which hindered its application at the industrial level. Most importantly, the thermal and chemical stability of MOFs is a bottleneck which requires to be overcome. Out of an excess of 2000 MOF matrix synthesized and analyzed, very few could withstand a temperature in excess of 300^oC. The frameworks collapse and showed low robustness at moderate to high temperatures. Moreover, frameworks also showed less immunity under aqueous and various organic mediums. Qualitatively as well as quantitatively speaking, same MOF synthesized at same conditions (keeping constant stoichiometry) following same recipes at times tend to yield products with varying percentage purities. Since, percentage yields and product purities of different batches vary; care must be taken during synthesis and post-synthesis treatments. It is also observed that MOFs undergoing adsorption mechanism in pressure swing adsorption (PSA) column undergo physical deformation after a few cycles or swings. The effect of high pressure is also a cause of concern before they can be approved to be industrially more viable.

In order to ultimately find the separation factor of carbon dioxide and methane, one must understand their molecular behavior. The carbon dioxide molecule is linear and centro-symmetric. The two C-O bonds are equivalent and are short in length of about 116.3 pm, which is consistent with double bonding. Since it is centro-symmetric, the molecules have no electrical dipole. Consistent with this fact, only two vibrational bands are observed in the Infra Red spectrum – an anti-symmetric stretching mode at 2349 cm^{-1} and a bending mode near

666 cm^{-1}. There is also a symmetric stretching mode at 1388 cm^{-1} which is only observed in the Raman spectrum.

2.2 CO_2 vs. CH_4: Molecular Comparison

Methane is a tetrahedral molecule with four equivalent C-H bonds. Its electronic structure is described by four bonding molecular orbitals (MOs) resulting from the overlapping of the valence orbitals on C and H. The lowest energy MO is the result of the overlap of the 2s orbital on carbon with the in-phase combination of the 1s orbitals on the four hydrogen atoms. Above this level in energy is a triply degenerate set of MOs that involve overlapping of the 2p orbitals on carbon with various linear combinations of the 1s orbitals on hydrogen. The resulting "three-over-one" bonding scheme is consistent with photoelectron spectroscopic measurements.

Meanwhile, CO_2 has a significant quadrupole moment (-1.4×10^{-35} Cm) that induces specific interactions with adsorbents (molecular orientation, hydrogen bonding…), CH_4 has no specific moment. It would thus seem that polar molecules have a distinct effect on the framework flexibility. Other significant physical properties are listed in the table below. A quick look at it suggests several similarities in liquid molar volume, kinetic diameter and polarizability, the presence of quadrupole moment being the only significant difference. Hence, the two gases cannot be disregarded as being totally dissimilar, but only partially so.

Table 2.1: Physical Properties Table

Gas	Mol. Wt.	Liqiud molar volume ($cm^3\ mol^{-1}$)	Kinetic dia. (Å)	Polarizability ($\times 10^{-25}\ cm^3$)	Dipole moment ($\times 10^{18}$ esu. Cm)	Quadrupole moment ($\times 10^{-40}\ C.m^2$)
CH_4	16	37.3	3.8	26.0	0.0	0.0
CO_2	44	33.3	3.3	26.3	0.0	14.3

2.3 MOFs as a tool for CO_2+CH_4 separation

Metal organic frameworks (MOFs) have been recognized as a new class of nanoporous materials that have shown many potential advantages over the traditional adsorbents. MOFs are synthesized using organic ligands and metal clusters that self-assemble in order to form crystalline materials with well-defined structures having controlled pore size, high surface area, and desired chemical functionalities [11–15]. These attractive properties make MOFs suitable for gas separation and storage [16–21]. MOFs have also been reported as potential adsorbents for separating CO_2 from CH_4. Couck et al. improved the selectivity of CH_4/CO_2 separation by functionalizing the MIL-53(Al) metal organic framework with amino groups [22]. Bae et al. reported a selectivity of ~30 for CO_2 over CH_4 for a mixed-ligand MOF. Moon et al. demonstrated that a MOF with unsaturated Mn^{II} sites has a much higher adsorption capacity for CO_2 than for CH_4. Similarly, selective adsorption of CO_2 over CH_4 with equilibrium selectivity of ~17 is obtained with a carborane-based MOF containing co-ordinatively unsaturated metal sites [23]. Moreover, extrudates with the commercially available $Cu_3(BTC)_2$ MOF were evaluated in vacuum pressure swing adsorption units for CO_2/CH_4 separation. This adsorbent showed a selectivity of 4–6 at pressures of 0.1–3 bar and a very high capacity for CO_2 (6.6 mol/kg at 2.5 bar and 303 K) [41]. These results have shown that MOFs with open metal sites can improve the separation of (quadru) polar/nonpolar gas pairs such as CO_2/CH_4.

CHAPTER 3

THEORY ON ADSORPTION ISOTHERMS

This chapter focuses on the industrial adsorption processes namely Pressure Swing Adsorption and Temperature Swing Adsorption cycles. It also briefly describes a few contemporary Adsorption Isotherms which were considered in the research.

3.1. Industrial Adsorption Processes

Industrial adsorption processes are usually cyclic processes in which adsorption and desorption steps of the sorbent material occur alternately. Often it's desorption or the regeneration step which is the most crucial since it essentially determines the period and the energetic efficiency of the cycle. The maximum efficiency that a cyclic adsorption process can offer for any given set of operating conditions is defined by the adsorptive loading that is in equilibrium with the feed fluid. There are several factors that reduce the practical (or "operating") adsorption: mass-transfer resistance, deactivation, and incomplete regeneration (or *desorption*). The severity of regeneration indicates how closely the dynamic capacity of an adsorbent resembles that of fresh, virgin material. Regeneration, or reversal of the adsorption process, requires a certain reduction in the driving force for adsorption. This is accomplished by increasing the equilibrium driving force for the adsorbed species from the solid to the surrounding fluid. This brings us to the topic of Pressure Swing Adsorption (PSA) and Temperature Swing Adsorption (TSA).

3.1.1 Pressure Swing Adsorption

Pressure swing adsorption processes make use of the fact that under high pressure, gases tend to be adsorbed more and vice a versa. In pressure-swing adsorption (PSA) processes, desorption takes place at a pressure which is much lower than that at adsorption. Reduction of pressure is used to shift the adsorption equilibrium and hence affect regeneration of the adsorbent.

Figure 3.1 shows a simplified pressure-swing cycle. Feed fluid with an adsorbate at a molar concentration of $y_1 = p_1 / P_1$ is passed through an adsorbent at conditions T_1, P_1, and the

adsorption step continues till the equilibrium loading n_1 is achieved with y_1. Next, the total pressure is brought down to P_2 during the depressurization (or blow-down) step. Although the partial pressure in equilibrium with n_1 is still p_1, there is a concentration driving force of $y_2 = p_1 / P_2 > y_1$ for desorption into any fluid containing less than y_2. By passing a fluid across the adsorbent in the purge step, adsorbate is swept away and the equilibrium proceeds along the isotherm to a point such as y_1, n_2. At this moment, the adsorbent is re-pressurized to P_1. The new equilibrium y_3, n_2 depicts the best quality product that can be produced from the adsorbent at a regeneration loading of n_2. The adsorption step is again repeated. The differential loading, $n_1 - n_2$, is the maximum loading that can be achieved for this pressure-swing cycle operating between a feed with y_1 and a product containing a molar concentration y_3 of the adsorbate. The regeneration fluid will have an average concentration between y_2 and y_1 and will therefore have accomplished concentration of the adsorbate in the regenerant gas.

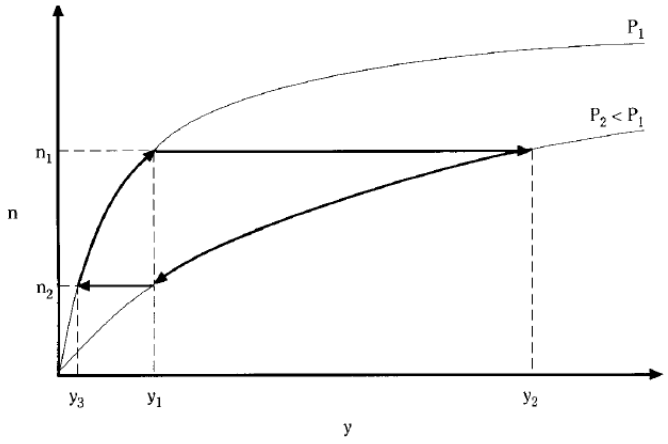

Figure 3.1: loading vs concentration plot depicting PSA

If a gas mixture, for example air, is passed under pressure through a vessel that contains an adsorbent bed of zeolite attracting nitrogen more strongly than it does oxygen, part of it or all of the nitrogen will stay in the bed, and the gas that comes out of the vessel will be enriched in oxygen. When this bed cannot adsorb any more nitrogen, it is regenerated by reducing the pressure, thus releasing the adsorbed nitrogen. It is now ready for another cycle of producing such oxygen enriched air. Use of two adsorbent vessels permits near-continuous production of the target gas. It also allows the so-called pressure equalization, where the gas leaving the vessel

being depressurized is used to pressurize the second vessel. This results in significant energy saving, and is hence a common industrial practice. Thus, in a PSA process cycle, regeneration can be achieved by depressurization that ultimately reduces the partial pressure of the adsorbates to allow desorption.

Low capacities at high concentrations ask for shorter cycle times for a reasonably sized beds (seconds to minutes). These short cycle times can be attained because particles of the adsorbent respond quickly to changes in pressure. Major applications for PSA processes include purification and applications where the contaminants are present at high concentration (bulk separations).

3.1.2 Temperature Swing Adsorption

A temperature-swing or thermal-swing adsorption (TSA) process is one in which desorption takes place at a temperature that is much higher than adsorption. The elevation of temperature is hence, used to shift the adsorption equilibrium and affect regeneration of the adsorbent.

It can be better understood by the process in Figure 3.2. The feed fluid having an adsorbate at a partial pressure of p_1 is made to pass through an adsorbent at temperature T_1. This adsorption step continues till the equilibrium loading n_1 is achieved with p_1. Further, the adsorbent temperature is raised to T_2 (heating step) so that the partial pressure which is in equilibrium with n_1 is increased to p_2, thus creating a partial pressure driving force for it's desorption into any fluid which will contain less than p_2 of the adsorbate. By passing a purge fluid across the adsorbent, adsorbate is now swept away. Equilibrium now proceeds along the isotherm to a point say p_1, n_2. Also, roll-up of the adsorbed-phase concentration can occur whilst heating, such that in some regions, p_2 may the condensation pressure of the component, resulting in a condensed liquid phase formed temporarily in the particles [24]. During the cooling step, the adsorbent temperature is returned back to $T1$. The new equilibrium p_3, n_2 depicts the best-quality product that could be produced from the adsorbent at a regenerated loading of n_2. The adsorption step is now repeated over. The differential loading, n_1-n_2, is the maximum amount of loading that can be achieved for such a TSA cycle which is operating between a feed containing p_1 at temperature T_1, regeneration at T_2, and a product containing a partial pressure p_3 of the adsorbate. The

regeneration fluid would contain an average partial pressure that is between p_2 and p_1 and therefore would have accomplished the concentration of the adsorbate in the regenerant fluid.

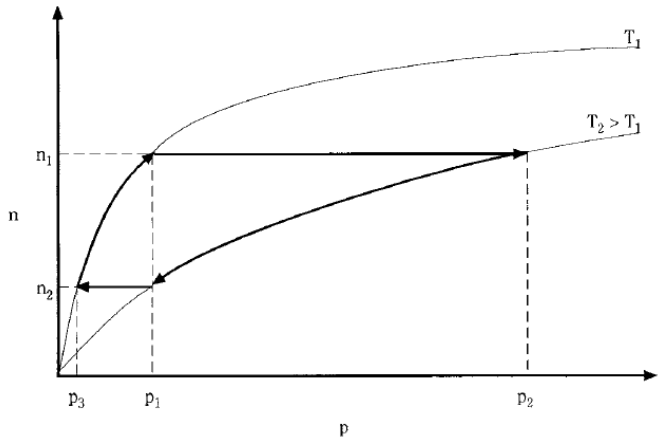

Figure 3.2: Loading vs. partial pressure plot depicting TSA

In TSA cycles, the heating step provides the required thermal energy which is necessary to raise the adsorbate, adsorbent, and adsorber temperatures, so as to desorb the adsorbate, and make up for the heat losses. TSA regeneration process is classified as (1) heating-limited (or stoichiometric limited) i.e. when transfer of energy to the system is limiting, or (2) stripping-limited (or equilibrium-limited) i.e. when transferring adsorbate away is limiting. Heating is done either by direct contact of the adsorbent with the heating medium (external heat exchange to a purge gas) or by other indirect means (heating elements, coils, or panels inside the adsorber). Direct heating is used most commonly, especially for the stripping-limited kind of heating. Indirect heating can also be considered for stripping-limited heating, but its sheer complexity limits its practicality to only heating-limited regeneration where the purge gas is in short supply.

PSA vs. TSA: Since in TSA cycles high temperature can be used, that results in thorough desorption, they are characterized by low residual loadings and hence high operating loadings. Such high capacities at low concentrations account for long cycle times in a reasonably sized adsorber (hours to days). Long cycle times are required because the particles of adsorbent respond pretty slowly to changes in the gas temperature. Most applications of TSA are in systems which have adsorbates are present at low concentration, such as drying, and in which species are more strongly adsorbed, such as sweetening, CO2 removal, and pollution control.

Although when PSA operating costs are too high, TSA is often less expensive to operate, despite its high initial cost of buying. Also, when the high product purities are not achievable with PSA, TSA may be suitable.

3.2 Adsorption Isotherms

Adsorption of a pure component of gas on a solid at equilibrium can be represented by the following function:

$$N = f(P, T) \quad \textbf{(3.1)}$$

Where, N is the amount adsorbed in cc STP per gm, P is the pressure and T is temperature.

At constant temperature, the amount of gas adsorbed onto a solid surface is only a function of P and is known as adsorption isotherm. During the process of adsorption, adsorbate molecules get attached to the adsorbent surface physically due to van der Waal's forces of attraction.

$$\text{Adsorbate} + \text{Adsorbent} \underset{\text{desorption}}{\overset{\text{Adsorption}}{\rightleftharpoons}} \text{Adsorption}$$

$$A + B \rightleftharpoons AB$$

According to Le-Chatelier principle, the direction of equilibrium would shift in that direction where the stress can be relieved. In case of application of excess of pressure to the equilibrium system, the equilibrium will shift in the direction where the number of molecules decreases. Since number of molecules decreases in forward direction, with the increases in pressure, forward direction of equilibrium will be favored.

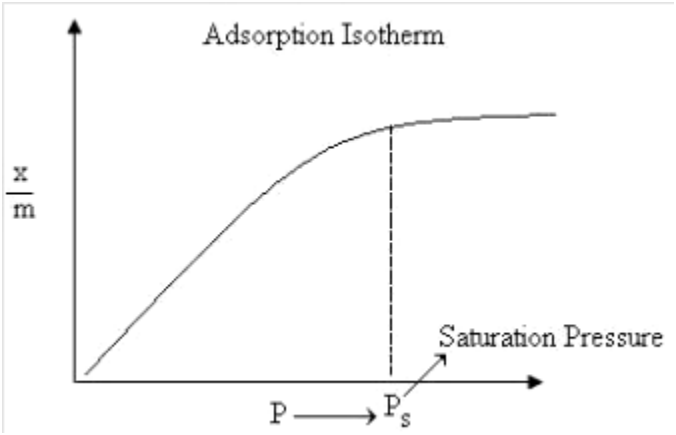

Figure 3.3: Basic Adsorption Isotherm

From the graph, we can predict that after saturation pressure Ps, adsorption does not occur anymore. This can be explained by the fact that there are limited numbers of vacancies on the surface of the adsorbent. At high pressure a stage is reached when all the sites are occupied and further increase in pressure does not cause any difference in adsorption process. At high pressure, Adsorption is independent of pressure.

3.2.1 Types Of Isotherms

The great majority of isotherms observed to-date can be classified into five types as shown in Figure below.

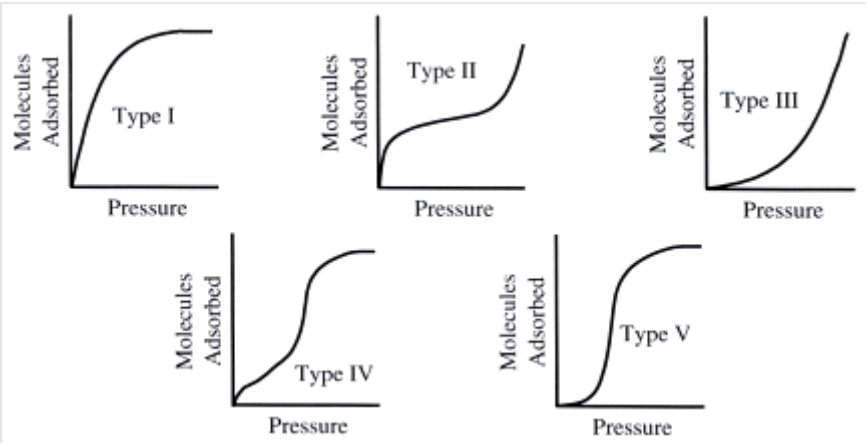

Figure 3.4: The five types of adsorption isotherms described by Brunauer[26]

Type I: This type of isotherm arises when only one type of adsorption site is present. It depicts monolayer adsorption. Initially, surface fills randomly then eventually the solid starts to saturates when surface gets up filled or pores get filled up for a porous material then the adsorption becomes constant and don't increase with increasing pressure and the pressure is termed as Saturation pressure.

Type II: This type arises when there is more than one adsorption site present on the solid. At first initial rapid adsorption takes place when first site is saturated second starts to fill up. Second site could be a second monolayer, a second site on the surface. In porous material, it can be a second type of pore.

Type III: This type arises when there are strong attractive interactions between the molecules leading to condensation. Initially, no adsorption takes place when pressure increases it leads to nucleation eventually liquids condense on the surface.

Type IV: At lower pressure region of graph is quite similar to Type II. This explains formation of monolayer followed by multilayer. The saturation level reaches at a pressure below the saturation vapor pressure .This can be explained on the basis of a possibility of gases getting condensed in the tiny capillary pores of adsorbent at pressure below the saturation pressure of the gas.

Type V: It is a another case for attractive interaction initially no adsorption takes place later nucleation starts which leads to formation of liquid drops and coverage saturates when no more space is left to hold adsorbate.

Type I and II are the most frequently encountered in separation process. Many theories and models have been developed to interpret these types of isotherms.

3.2.2 Isotherm Models

Important isotherm models are discussed in this section.

3.2.2.1 Freundlich Adsorption Isotherm

In 1909, Freundlich gave an empirical expression representing the isothermal variation of adsorption of a quantity of gas adsorbed by unit mass of solid adsorbent with pressure. This equation is known as Freundlich adsorption isotherm or Freundlich adsorption equation. The Freundlich adsorption isotherm is mathematically expressed as:

$$\frac{x}{m} = KP^{\frac{1}{n}} \tag{3.2}$$

Also written as,

$$\log(\frac{x}{m}) = \log k + (\frac{1}{n}) \log P \tag{3.3}$$

Or

$$\frac{x}{m} = Kc^{\frac{1}{n}} \tag{3.4}$$

3.2.2.2 Langmuir Adsorption Isotherm

When Freundlich isotherm failed at higher temperature Irving Langmuir in 1916 derived a simple adsorption isotherm, on theoretical considerations based on kinetic theory of gases. This is named as Langmuir adsorption isotherm. The *Langmuir equation* relates the coverage or adsorption of molecules on a solid surface to gas pressure or concentration of a medium above the solid surface at a fixed temperature. The equation is stated as:

$$\theta = \frac{\alpha P}{1 + \alpha P} \tag{3.5}$$

Where, θ is the fractional coverage of the surface, P is the gas pressure or concentration, α is a constant. The constant α is the *Langmuir adsorption constant* and increases with an increase in the binding energy of adsorption and with a decrease in temperature.

The following assumptions are used by Langmuir while deriving the equation:

- Adsorption occurs on a fixed number of sites.
- Each site can only take one adsorbate molecule
- All sites are energetically equivalent
- Interaction between adsorbed molecules are neglected as they are assumed to be small compared to sorbate/sorbent interactions
- Dynamic equilibrium exists between adsorbed gaseous molecules and the free gaseous molecules.

3.2.2.3 Freundlich-Langmuir Isotherm

A combined equation of Freundlich and Langmuir was proposed in the following form:

$$q = \frac{(qm)bP^n}{1+bP^n} \tag{3.6}$$

3.2.2.4 Dual Site Langmuir (DSL) Isotherm[26]

The Dual Site Langmuir (DSL) model is a four-parameter isotherm, distinguishing two categories of different active sorption sites in the adsorbent, each one following a Langmuir adsorption behaviour.

$$N = \frac{N_1^{\max} b_1 P}{1+b_1 P} + \frac{N_2^{\max} b_2 P}{1+b_2 P} \tag{3.7}$$

Where, N_i^{max} and b_i denotes saturation capacity and affinity parameters for sites of type 'i' respectively. The temperature dependency is included through affinity parameters via

$$b_i = b_i^0 \exp\left[\frac{-\Delta h_{ads}^{(i)}}{R}\left(\frac{1}{T}-\frac{1}{T_0}\right)\right] \quad \textbf{(3.8)}$$

Where, b_i^0 is the affinity at reference at T_0 and $-\Delta h_{ads}^{(i)}$ is the enthalpy of adsorption on site *i* with respect to temperature T_0 . The Henry's constant in this case is given by

$$H = N_1^{\max} b_1 + N_2^{\max} b_2 \quad \textbf{(3.9)}$$

3.2.2.5 Virial Isotherm

Based on virial equation of state of the form

$$\frac{\pi a}{RT} = 1 + \frac{b}{a} + \frac{c}{a^2} \quad \textbf{(3.10)}$$

For the two-dimensional surface phase the virial isotherm model can be derived and is represented by

$$\ln(P/N) = k + bN + cN^2 \quad \textbf{(3.11)}$$

e^{-k} Is the Henry constant and is related to the gas-solid interactions only. The other higher coefficients *viz. b*, *c* etc. are called as second and third Virial coefficients respectively. The temperature dependency of Virial coefficients is given by

$$k = k_0 + \frac{k_1}{T} \quad \textbf{(3. 12)}$$

$$b = b_0 + \frac{b_1}{T} \quad \textbf{(3. 13)}$$

$$c = c_0 + \frac{c_1}{T} \quad \textbf{(3. 14)}$$

The physical interpretations of the virial coefficients are strictly valid only for homogeneous adsorbents at low coverage. Since virial equation is open-ended, there is no limit on the amount adsorbed as the pressure is increased. But, this can lead to erroneous results if the virial equation is extrapolated beyond the range of data. However, within the temperature and pressure limits of the data, virial equation is flexible and thermodynamically consistent. The virial equation is also reliable to calculate Henry's law constants with good accuracy. In fact in a virial domain plot [ln(P/ N) vs. N] or [ln(f / N) vs. N] the intercept is k and is directly related to Henry constant. Henry's constant H is given by

$$H = e^{-k} \tag{3.15}$$

3.2.2.6 Virial-Langmuir (V-L) Isotherm

The Langmuir equation usually assumes energetic homogeneous surface, rarely possible in realistic situation. On the other hand, virial equation is flexible, thermodynamically correct and describes the heterogeneity of the surface. However, the virial model does not explain the saturation at high pressure, a phenomena observed in many cases. To overcome this limitation, virial model is modified for an additional term to introduce saturation behavior at high pressure. The regular isotherm is given by Eq. (3.11) and the modified equation known as Virial-Langmuir isotherm is given by

$$P = \frac{N}{H}\left[\frac{N^{\max}}{N^{\max} - N}\right]\exp[bN + cN^2] \qquad (N < N^{\max}) \tag{3.16}$$

Here, H is Henry constant; b, c are virial coefficients; N_i^{max} is the saturation capacity. If all the virial coefficients in the Eq. (3.16) are zero, the above expression reduces to the well known Langmuir equation. The temperature dependency of the parameters H, b and c in this case is given by the following expressions similar to those as described in the preceding paragraph. Saturation capacity N_i^{max} is also expressed with similar functionality.

$$N^{\max} = \beta^{\max,0} + \frac{\beta^{\max,1}}{T} \tag{3.17}$$

3.2.2.7 Gibbs' Adsorption Isotherm

For the sake of clarity ideal bulk gas phase is used in the following equations. However, without any loss of generality, pressure can be replaced by the fugacity of a real gas mixture at any stage. From the following equation,

$$\mu_i^g = \mu_i \qquad \text{Or} \qquad d\mu_i^g = d\mu_i \tag{3.18}$$

The chemical potential in the surface phase given in terms of the bulk gas phase properties is,

$$d\mu_i = RTd\ln(y_i P) \qquad \text{(constant } T\text{)} \tag{3.19}$$

From the fundamental property relations, any molar property M for the adsorbed phase can be written as,

$$N.M = M\{T, \pi, N_1, N_2, ...\} \tag{3.20}$$

The total differential is

$$d(N.M) = \left[\frac{\partial(N.M)}{\partial \pi}\right]_{T,N_i} d\pi + \left[\frac{\partial(N.M)}{\partial T}\right]_{\pi,N_i} dT + \sum_i \left[\frac{\partial(N.M)}{\partial n_i}\right]_{\pi,T,N_{j\neq i}} dN_i \tag{3.21}$$

Gibbs-Duhem relation follows Eq. 3.20 and is given as

$$\left[\frac{\partial M}{\partial \pi}\right]_{T,x} d\pi + \left[\frac{\partial M}{\partial T}\right]_{\pi,x} dT - \sum_i x_i d\left[\frac{\partial(N.M)}{\partial n_i}\right]_{\pi,T,N_{j\neq i}} = 0 \tag{3.22}$$

Using g for the property M in Eq. (3.21) together with Eq. (3.18), the Gibbs' adsorption isotherm is given by

$$-a.d\pi + RT\sum x_i d\ln(y_i P) = 0 \qquad \text{(constant } T\text{)} \tag{3.23}$$

Substituting $a = A/n$,

$$-A.d\pi + RT\sum N_i d\ln(y_i P) = 0 \qquad \text{(constant } T\text{)} \tag{3.24}$$

For a single component system the equation simplifies to

$$-A.d\pi + RT.N.d\ln P = 0 \qquad \text{(constant } T\text{)} \qquad \textbf{(3.25)}$$

This is called as the Gibbs' adsorption isotherm in adsorption literature [29].

Spreading Pressure

Integrating Eq. (3.23) from zero pressure to a pressure P,

$$\psi = \frac{\pi.A}{RT} = \int_0^P \frac{N}{P}.dP \qquad \textbf{(3.26)}$$

The quantity ψ has the units of moles per unit mass of adsorbent. It is called reduced spreading pressure and is often used synonymously with π. At $P = 0$, there is no adsorption and the spreading pressure is zero.

The spreading pressure is not an experimentally measurable quantity. Thus, relations like Eq. (3.26) are used to calculate its value for a pure gas adsorption. More cumbersome exercise is necessary to find its value for multi component mixtures [22].

3.3 Ideal Adsorbed Solution Theory (IAST)

A solution thermodynamic approach yields the following phase equilibrium relation for equality of fugacities in bulk and adsorbed phases.

$$y_i P \hat{\phi}_i^{gas} = x_i \gamma_i P_i^0 \qquad \textbf{(3.27)}$$

Where, y_i is bulk gas mole fraction, P is the pressure, $\hat{\phi}_i^{gas}$ is fugacity coefficient of bulk gas to account for non-ideality, x_i is adsorbed phase mole fraction, γ_i is activity coefficient in adsorbed phase (to account for non-ideal adsorbate mixture) and P_i^0 is pressure at the standard state.

A convenient standard state is pure gas at same temperature and spreading pressure as that of the mixture. If the adsorbate mixture is ideal (IAST) and neglecting gas phase non-ideality Eq. 3.27 simplifies to

$$y_i P_i^{gas} = x_i P_i^0 \tag{3.27}$$

With this phase equilibrium relations along with an equation for total amount adsorbed (N), one can predict binary gas adsorption equilibria (i.e. finding partial amount adsorbed N_i from a given gas mixture of mole fraction y_i at T and P. For example in case of binary equilibrium, the following eight equations need to be solved.

$$x_1 P_1^0 = y_1 P \tag{3.28}$$

$$x_2 P_2^0 = y_2 P \tag{3.29}$$

$$\xi_1\{P_1^0\} = f_1^0\{P_1^0\} \tag{3.30}$$

$$\xi_2\{P_2^0\} = f_2^0\{P_2^0\} \tag{3.31}$$

$$\xi_3\{P_1^0, N_1^0\} = f_3^0\{P_1^0, N_1^0\} \tag{3.32}$$

$$\xi_4\{P_2^0, N_2^0\} = f_4^0\{P_2^0, N_2^0\} \tag{3.33}$$

$$x_1 + x_2 = 1 \tag{3.34}$$

$$\frac{1}{N} = \frac{x_1}{N_1^0} + \frac{x_2}{N_2^0} \tag{3.35}$$

The functionalities denoted by ξ_i in the above equations for amounts adsorbed N_i^0 at standard state and spreading pressure ψ can be obtained from pure gas equilibrium data [88].

CHAPTER 4

EXPERIMENTAL WORKS AND DATA RETRIEVAL

This chapter illustrates MOF synthesis methods for specifically Cu-BTC, Cr-BDC. Finally, data retrieval methods are also discussed.

4.1 Synthesis of Cu-BTC

Cu-BTC or HKUST-1 was first reported by Chui et al. [50]. This method reported by Liu et al. and is a modification of previous works by Roswell and Yaghi [51]. 1, 3, 5-benzenetricarboxylic acid (1.0 g) is dissolved in 30 ml of a 1:1 mixture of ethanol/N, N-dimethylformamide (DMF). In another flask, Copper (II) Nitrate trihydrate (2.077 g) is dissolved in 15 ml water. The two solutions are then mixed and stirred for 10 min. They are then transferred into Teflon-lined stainless steel autoclave and heated at 373 K for 10 hours. The reaction vessel is cooled to room temperature normally. The resulting blue crystals are isolated by filtration and extracted with methanol overnight using a Soxhlet extractor to remove solvated DMF. The product is then dried at room temperature.

4.2 Synthesis of Cr-BDC

Cr-BDC or MIL-101 is synthesized hydrothermally following the published work of Ferey et al.[52]. The reaction is carried out in a Teflon lined stainless steel autoclave where a stoichiometric mixture of $Cr(NO_3)_3.9H_2O$, de-ionized water, 1,4-benzene dicarboxylic acid and HF is placed for 8 hrs at 493 K. Post-synthesis treatments of MIL-101 sample is crucial since significant amount of needle shaped colorless crystals of terephthalic acid (H_2BDC) is formed as a by-product.

4.3 Data Retrieval

All experimental data for our present study were retrieved from literature. 'Windig' software was used extensively for this purpose. Judicious interpolation and extrapolation was done wherever required. Model fitting was carried out using 'Microsoft Excel 2010' (version: 7.3.0.267). Various isotherm models were tried and tested on the experimental data to get the best fit. Model fit parameters were evaluated from model equations and the physical significance of each of the parameters was tried to be explained to understand the adsorption mechanism.

CHAPTER 5

RESULTS AND DISCUSSION

This chapter summarizes all the results. All experimental data for CH_4 and CO_2 obtained from literature is fit with standard isotherm models and compared. Interesting observations are made and explained in detail. The model fitting by suitable adsorption isotherm model has been done. Corresponding plots and model parameters are displayed. IAST study and the related selectivity graphs showing the variation in separation factor are likewise shown. Comparison of experimental data with simulation data at same condition is also made and elaborated.

5.1 Data Collection

Experimental Data collected on Adsorption of CO_2 and CH_4 on various MOFs (as reported over the years) is shown in the tables below:

Table 5.1: Experimental Data on Adsorption of CO_2 on various MOFs (as reported over the years)

Adsorbent	Pressure	Temperature	Loading	Isosteric Heat	$q_{st,0}$ (kJ mol^{-1})	Henry constant / H (mmol g^{-1} bar^{-1})	Ref
	P / (bar)	T / K	N / mmol g^{-1}	q_{st} / (kJ mol^{-1})			
MIL-53 (Al)	5, 10, 25	304	3.3, 8.2, 10.4	35-17			[42]
MIL-53 (Cr)	5, 10, 25	304	3.3, 8.0, 10	35-17			[42]
Cu-BTC	4, 12	298	10, 12.5				[36]
	0.97	313	1.6		14.5		[69]
Cu-BTC (sample b)	0.9	295	4.7			6.24	[38]
Cu-BTC (sample c)	10, 17.5	298	1.9				[38]
IRMOF-1		300			14.5		[69]
	0.8	298	0.57				[72]
IRMOF-3	1.03	313	1.25		19.5		[69]
	1	298	0.91				[72]
MIL-100	10, 60	303	9, 18.5	63-20	62		[45]
MIL-101 (Sample a)	10, 34	303	9, 25	32-18			[45]
MIL-101 (sample b)	10, 60	303	12, 32	32-18			[45]
MIL-101 (sample c)	10, 40	303	14.5, 34.8	45-25	44		[45]
MIL-47	5, 10, 20	304	6.3, 8.8, 11.4	25-20			[42]
	1	298	1.59				[72]
MOF-177	1	298	0.68				[72]
MOF-5	1.01	296	2.1				[73]

Table 5.2: Experimental Data on Adsorption of CH_4 on various MOFs (as reported over the years)

Adsorbent	Pressure	Temperature	Loading	Isosteric Heat	$q_{st,0}$ (kJ mol^{-1})	Henry constant / H (mmol g^{-1} bar^{-1})	Ref
	P / (bar)	T / K	N / mmol g^{-1}	q_{st} / (kJ mol^{-1})			
MIL-53 (Al)	5, 10, 25	304	2.2, 3.7, 6.0	17			[42]
MIL-53 (Cr)	5, 10, 25	304	2, 3.7, 5.8				[42]
Cu-BTC	6.25, 50, 100	303	5.63, 9.38, 9.5				[44]
	0.94	295	0.92				[76]
	1	295	0.6				[71]
	10, 50	298	5.35, 9.59				[78]
Cu-BTC	4, 12	298	2.3, 4				[36]
		300			12.5		[69]
Cu-BTC (sample b)	0.9	295	0.8			1.14	[38]
IRMOF-1		300			9.5		[69]
IRMOF-14	10, 50	298	3.57, 12.72				[78]
IRMOF-3		300			12.5		[69]
MIL-100	10, 60	303	3, 9.5	20-9	19	480	[45]
MIL-101	6.25, 50, 100	303	2.5, 7.19, 8.6				[44]
MIL-101 (Sample a)	10, 34, 80	303	3.7, 10, 14.5	18-10			[45]
MIL-101 (Sample b)	10	303	3.7	18-10			[45]
MIL-101 (Sample c)	10	303	3.7	18-10	18	580	[45]

Experimental Data on Adsorption of CH_4 and CO_2 as reported over the years reveal that for MIL-53(Al and Cr) the experiments have been carried out at the same lab [42] at three different Pressure conditions (5, 10 and 25 bar), keeping the temperature constant at 304 K. This is in agreement with our research objective to analyze the data for various optimum conditions.

Similarly for Cu-BTC, experimental data from three different labs are available [69], [36]. However for others [44], [71], [38] the data is available for either of the two (CO_2 & CH_4). For IRMOF-1 and IRMOF-3 experimental data for both the gases is available from only one source [69]. Likewise for MIL-101, data from a single lab [45] fulfils this criterion.

The loading data of CO_2 in all the above cases are considerably higher than those of CH_4. This is a clear indication of the fact that CO_2 is preferentially adsorbed and any process aimed at separating a mixture of CO_2 and CH_4 by adsorption, must do so by removal of CO_2 from the mixture. This is further supported by looking over at the Isosteric Column. Isosteric Heat of CO_2 is in general much higher than that of CH_4. Greater Isosteric heat indicates stronger bond formation, further implying that CO_2 is much more strongly adsorbed on the surface of the MOF.

5.2 Model Fitting

The source of pure gas adsorption data for this work was primarily taken from the extensive work done by Chowdhury et al. [84]. Although, many contemporary research works on gas adsorption of CO_2 and CH_4 on similar MOF surfaces have been undertaken by various research groups across the globe, but experimental data retrieved from the same lab under similar conditions was given paramount importance in the present context.

Model fitting was done for the data using Dual Site Langmuir and Virial Langmuir isotherm models on the two MOFs Cu-BTC and Cr-BDC for the gases CO_2 and CH_4 after data extraction.

The plot below shows the variation of the amount of CO adsorbed in Cr-BDC against fugacity for three different temperatures i.e. 293 K, 318 K and 358 K.

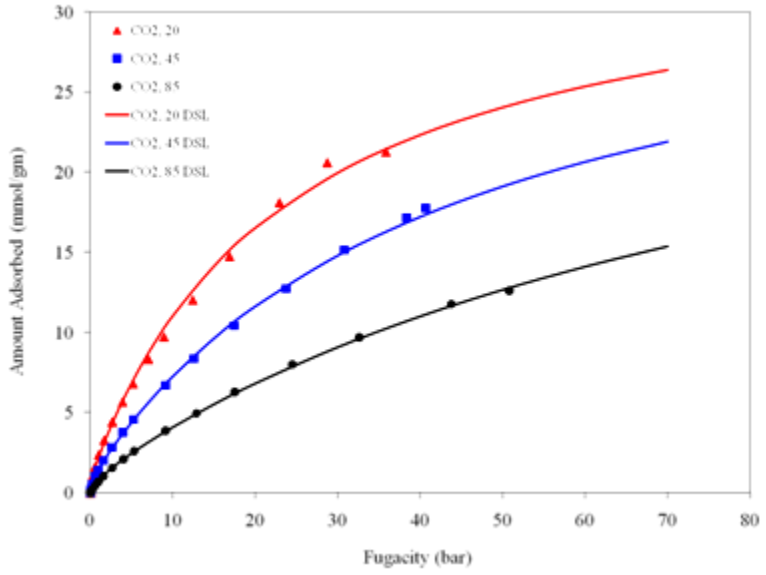

Figure 5.1: Dual Site Langmuir model fitted adsorption isotherm plot for CO_2 adsorption on Cr-BDC – amount adsorbed (N) vs. fugacity (f)

The reason fugacity is used in place of Pressure is because the pressure range and its variation is very high and goes up to nearly 100 bars. Hence, to incorporate any non-ideality that may arise out of it, pressure has been replaced by fugacity.

Also, the data when plotted was seen to be clustered for the lower fugacity values i.e. towards the lower portions of the graph. Hence to better visualize and to magnify the data plots of natural log of *f* over *N* were plotted.

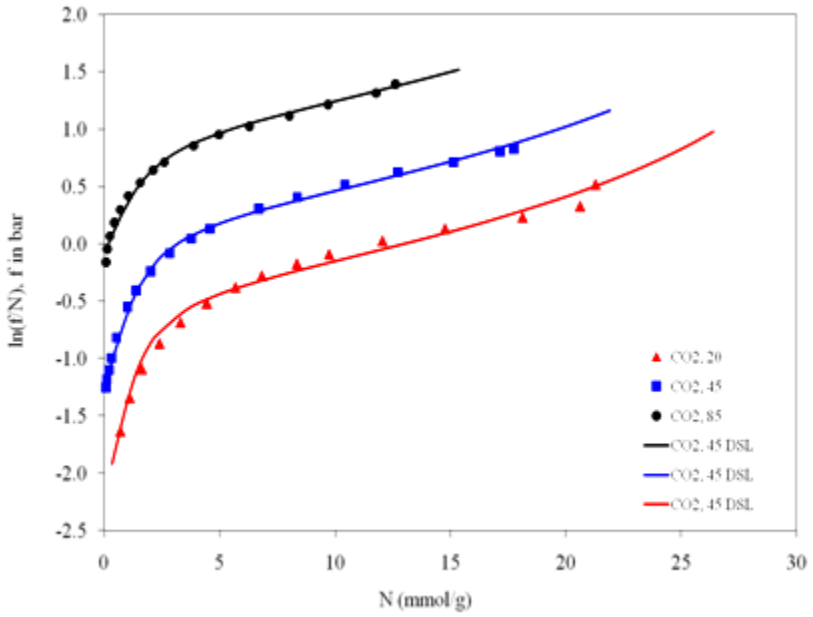

Figure 5.2: Dual Site Langmuir model fitted adsorption isotherm plot for CO_2 adsorption on Cr-BDC at low pressures – ln(f/N) vs. amount adsorbed (N)

Likewise the DSL model fitted adsorption isotherm plot for CH_4 adsorption on Cr-BDC - amount adsorbed (N) vs fugacity (f) and that of the natural log of *f* over *N* vs *N* plot are shown below.

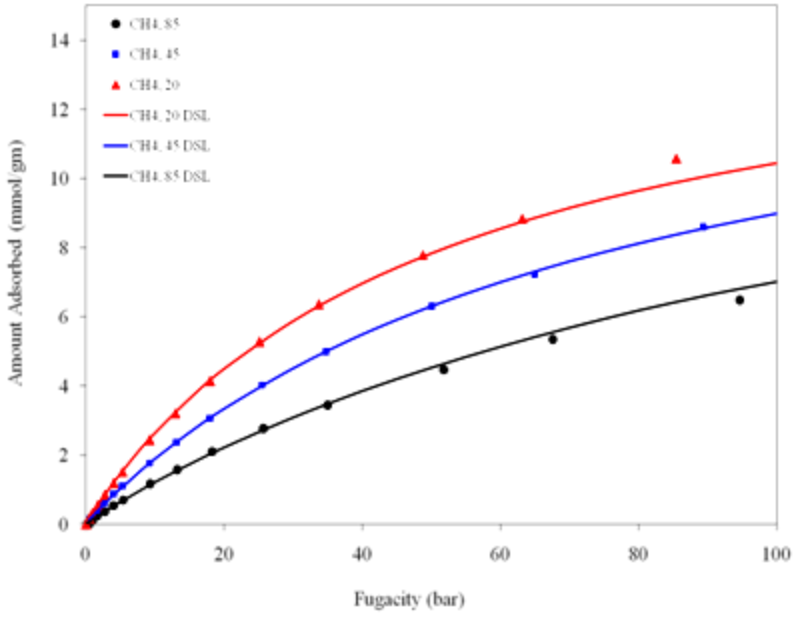

Figure 5.3: Dual Site Langmuir model fitted adsorption isotherm plot for CH_4 adsorption on Cr-BDC - amount adsorbed (N) vs. fugacity (f)

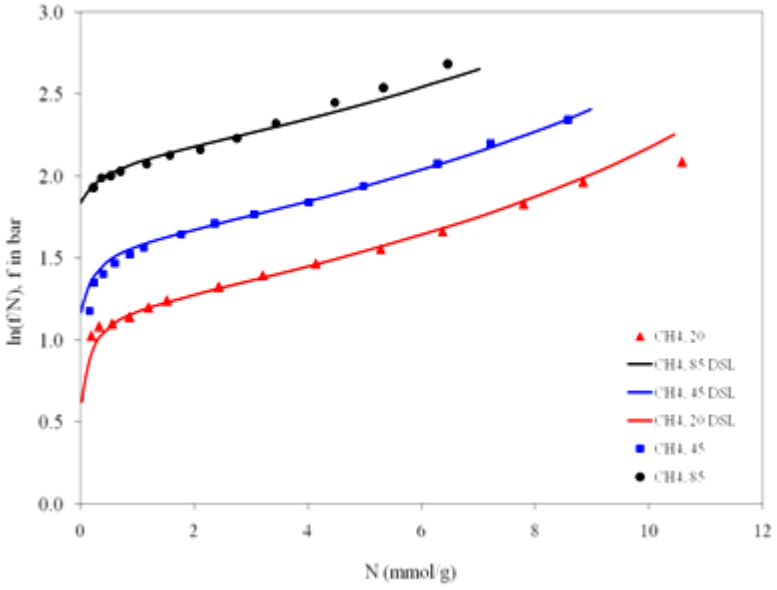

Figure 5.4: Dual Site Langmuir model fitted adsorption isotherm plot for CH_4 adsorption on Cr-BDC at low pressures – ln(f/N) vs. amount adsorbed (N)

Trend lines were drawn in excel by the curve fitting tool and the corresponding was found. After comparing the equation so obtained with the DSL equation, the various model parameters were found out. They are as shown in the table below.

Table 5.3: Dual Site Langmuir model fit parameters for CH_4 and CO_2 adsorption on Cr-BDC

Model Parameters	CH_4	CO_2
N_1^{max} (mmol g^{-1})	0.0716	0.9744
N_2^{max} (mmol g^{-1})	15.6817	34.044
b_1^0 (bar^{-1})	6.479	14.0436
b_2^0 (bar^{-1})	0.0248	0.0607
$-\Delta h_{ads}^{(1)}$ (kJ mol^{-1})	30.555	34.668
$-\Delta h_{ads}^{(2)}$ (kJ mol^{-1})	13.45	20.794

The reason Dual Site Langmuir has been used is because literature study reveals that Cr-BDC shows multiple types of adsorption sites. In this case, they are the Metallic sites and the Co-ordinatively Unsaturated Sites of CUS sites. This is supported by the significant curve of the leg shape in the ln(f/N) vs. N plots above. It shows higher rate of adsorption initially which falls quickly. It is evident also by observing the 1st and 2nd saturation loadings and also the 1st and 2nd heat of adsorption for both CO_2 and CH_4.The first saturation loading is significantly lower than the 2nd for both CO_2 and CH_4, However the heat of adsorption of 1st saturation loading is much higher than that of 2nd. All this can be attributed to the quicker initial filling up of the more strongly adsorbing, but much less in number, Metallic sites. Once the metallic sites get occupied, the CUS sites with significantly lower heat of adsorption but are large in number, start filling up, thus explaining the decreased rate of adsorption shown in the plots above in their latter portions.

Also, the saturation loading of CO_2 is higher than that of CH_4, once again implying that CO_2 is getting more strongly adsorbed than CH_4 as predicted earlier.

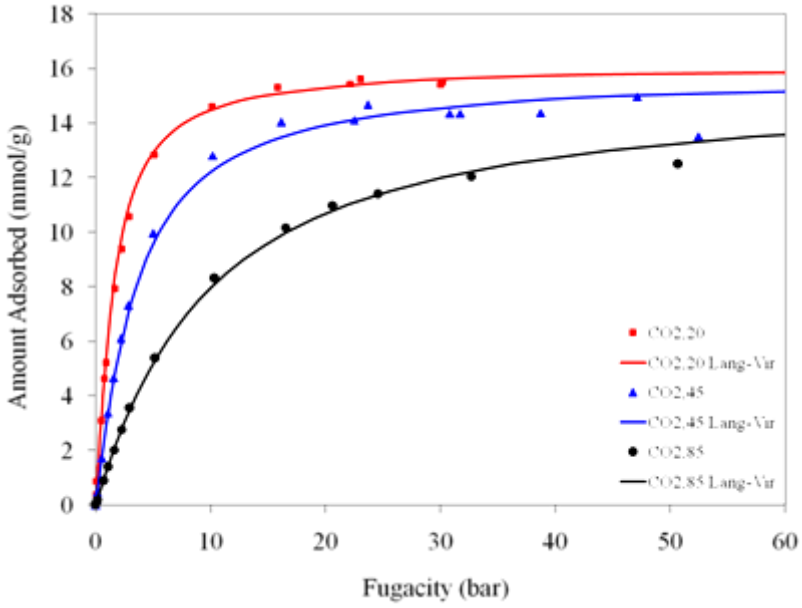

Figure 5.5**:** Langmuir Virial model fitted adsorption isotherm plot for CO_2 adsorption on Cu-BTC - amount adsorbed (N) vs. fugacity (f)

The data or pure gas sorption isotherm of CO_2 and CH_4 on Cu-BTC was likewise collected and similar graphs as with Cr-BDC were plotted. The model fitting this time, was done by Virial-Langmuir Isotherm.

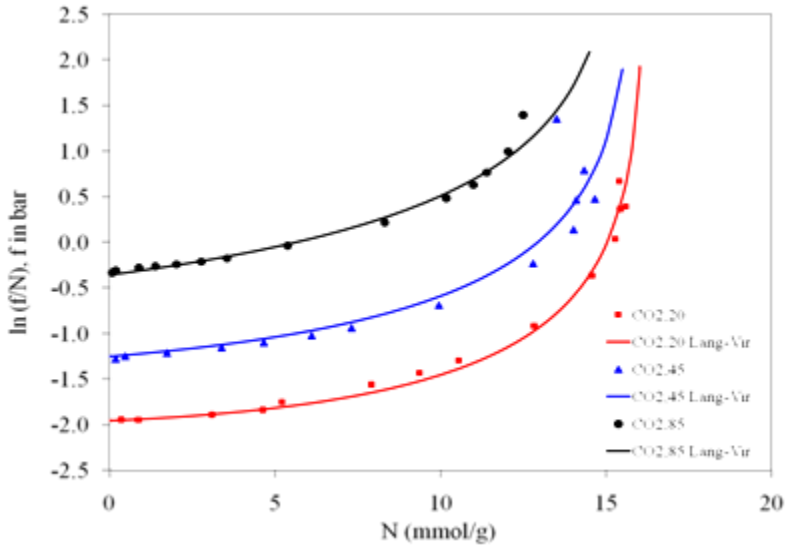

Figure 5.6: Langmuir Virial model fitted adsorption isotherm plot for CO_2 adsorption on Cu-BTC at low pressures – ln(f/N) vs. amount adsorbed (N)

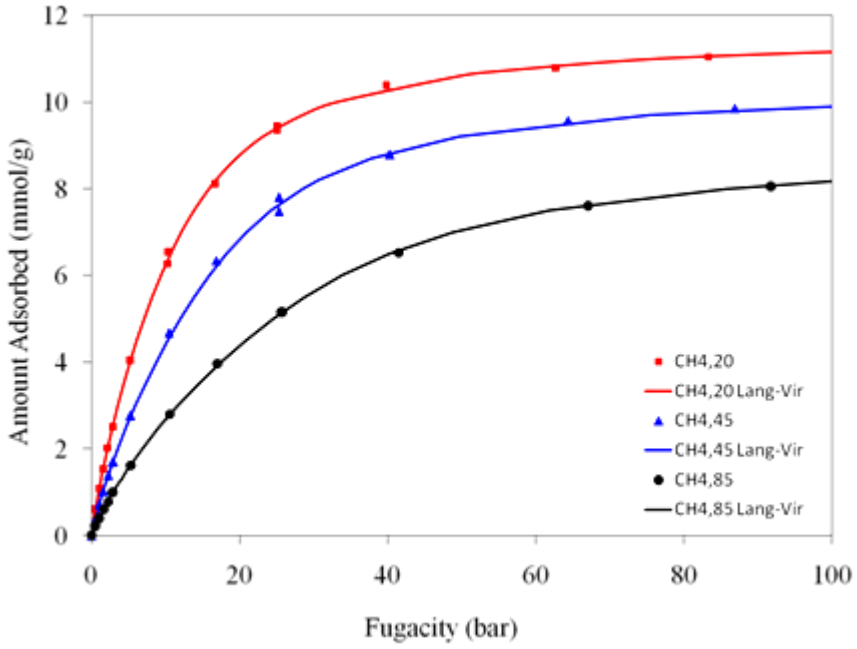

Figure 5.7: Langmuir Virial model fitted adsorption isotherm plot for CH_4 adsorption on Cu-BTC - amount adsorbed (N) vs. fugacity (f)

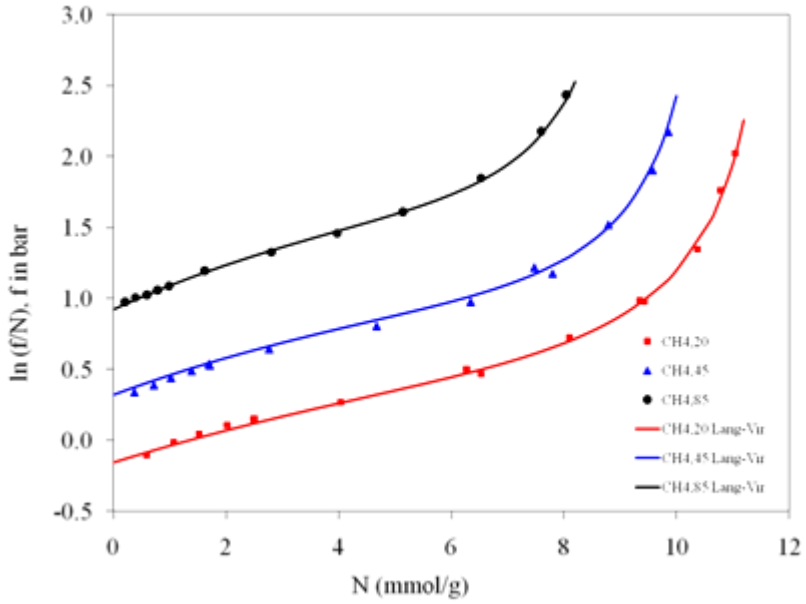

Figure 5.8: Langmuir Virial model fitted adsorption isotherm plot for CH_4 adsorption on Cu-BTC at low pressures – ln(f/N) vs. amount adsorbed (N)

Virial was chosen because the plot obtained didn't seem to appear to converge and appeared to closely resemble that of a polynomial. Also, Langmuir shows best results at lower pressure ranges as it deals with ideality. Hence to better fit the model, a combination of the two was used. Once again, by comparison of trend line the Virial coefficients were found out. A polynomial of degree two was considered, as even higher accuracy wasn't necessary. The model parameters found out are shown in the table below.

Table 5.4: Virial-Langmuir model fit parameters for CH_4 and CO_2 adsorption on Cu-BTC

Model Parameters	CH_4	CO_2
k_0	6.388	7.4805
k_1 (K)	-1931.21	-2774.01
b_0 (mmol^{-1} g)	0.239	0.454
b_1 (mmol^{-1} g K)	-59.2719	-157.539
c_0 (mmol^{-2} g^2)	-0.0679	-0.0687
c_1 (mmol^{-2} g^2 K)	17.1723	21.7839
$\beta^{max,0}$ (mmol g^{-1})	-4.0299	-8.2865
$\beta^{max,1}$ (mmol g^{-1} K)	4635	7642.651

5.3 Mixed Gas Behavior Study

Any realistic process development requires estimation and/or prediction of mixed gas adsorption behavior. Invariably, any industrial process involves mixture of gases to be separated. The practical demonstration of such a process at laboratory scale is an extremely cumbersome exercise and there is a scarcity on mixed gas experimental data in literature and more specifically on MOFs. It is pragmatic to gauge the efficiency of a particular adsorbent towards specific separation at the lab scale before being implemented at industrial level in a pressure swing adsorption (PSA) column.

This work is aimed at predicting the mixed gas adsorption behavior on MOFs. The paricular MOFs of our interest were Cu-BTC and Cr-BDC. Both of them have shown tremendous potential owing to their surface characteristics. However, a few important experimental

observations led to the selection of Cu-BTC for studying the mixed gas adsorption behavior. The reasoning are:

(a) Although the reported specific surface area of Cr-BDC (*ca*. 3000 m^2/gm) happens to be approximately 2 times than that of Cu-BTC (*ca*. 1500 m^2/gm), but the latter has shown better regeneration capacity after continuous cycles of pressure and temperature swings during pure gas adsorption isotherm measurements.

(b) The synthesis condition of Cr-BDC requires much higher temperature (*ca*. 220^{o}C) than Cu-BTC (*ca*. 95^{o}C), yielding significant by-products and necessitating a series of post synthesis treatments before being usable.

(c) Although both Cr-BDC and Cu-BTC has comparable final packing densities (*ca*. 0.5-0.7 gm/cc) but Cr-BDC samples show higher degree of crystal imperfections during synthesis and hence more prone towards rapid wear and tear when exposed to higher temperature and pressure in a packed bed adsorption column.

(d) Cu-BTC has a more uniform pore size distribution in micropore (<2 nm) regime whereas Cr-BDC is well known for mesoporosity.

Ideal Adsorption Solution Theory (IAST) can be effectively used to predict the mixed gas behavior, if the experimental pure gas isotherm data of the corresponding gases are known. Although MOFs are known for their incredible surface characteristics but a closer look at the literature would reveal variations in reported surface area and pore volume from lab to lab. Incidentally, it is very important to use the pure gas adsorption data of gases concerned (CO_2 and CH_4 in this case) reported from the same laboartory for realistic assessment on mixed gas behaviour.

Here, we report our findings on CO_2+CH_4 mixture using IAST model on Cu-BTC. The binary prediction is calculated from individual pure gas adsorption data of CO_2 and CH_4 on Cu-BTC. Figures 5.9 and 5.10 represents IAST predictions for CO_2+CH_4 mixture. The selectivity plots are shown in figures 2.13 and 2.14 respectively.

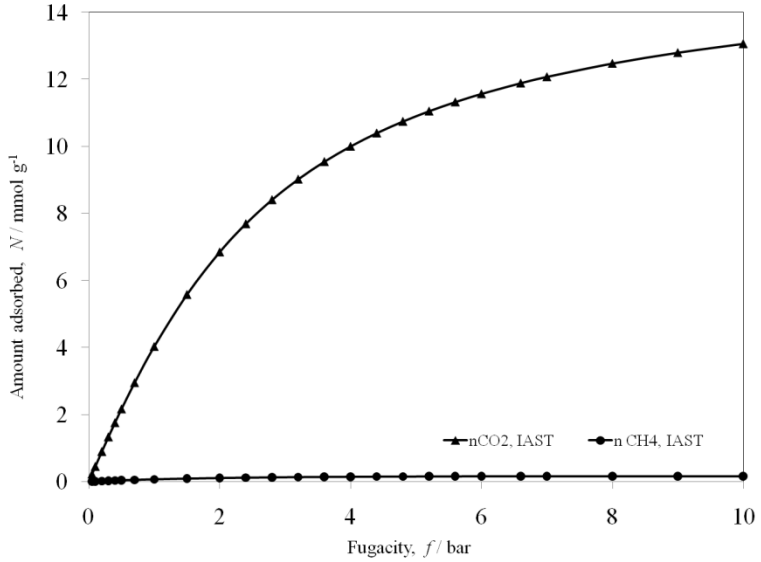

Figure 5.9: Variation of amount adsorbed from CO_2+CH_4 mixture at 305 K, y_{CH4} = 0.1

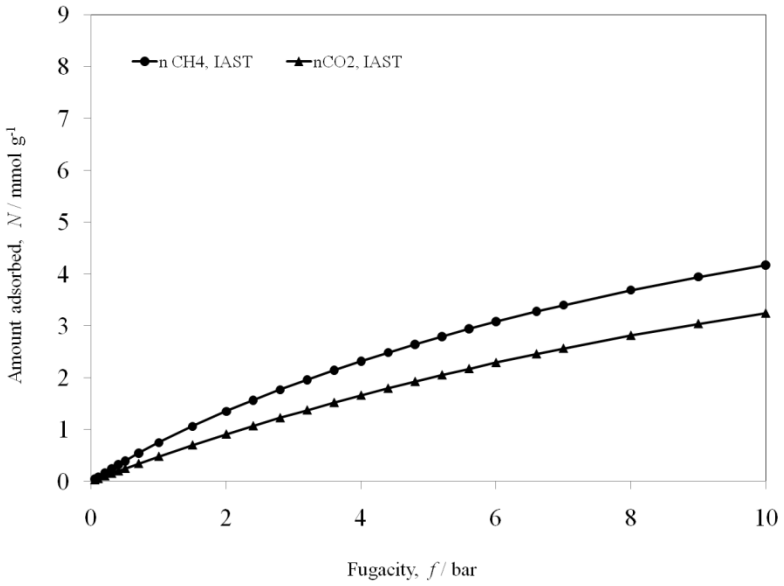

Figure 5.10: Variation of amount adsorbed from CO_2+CH_4 mixture at 305 K, y_{CH4} = 0.9

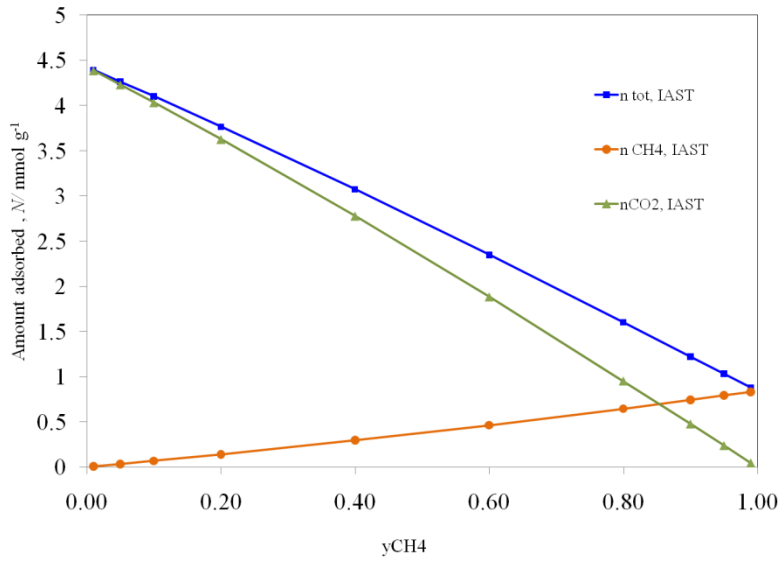

Figure 5.11: Variation of amount adsorbed from CO_2+CH_4 mixture at 305 K, P= 1 bar

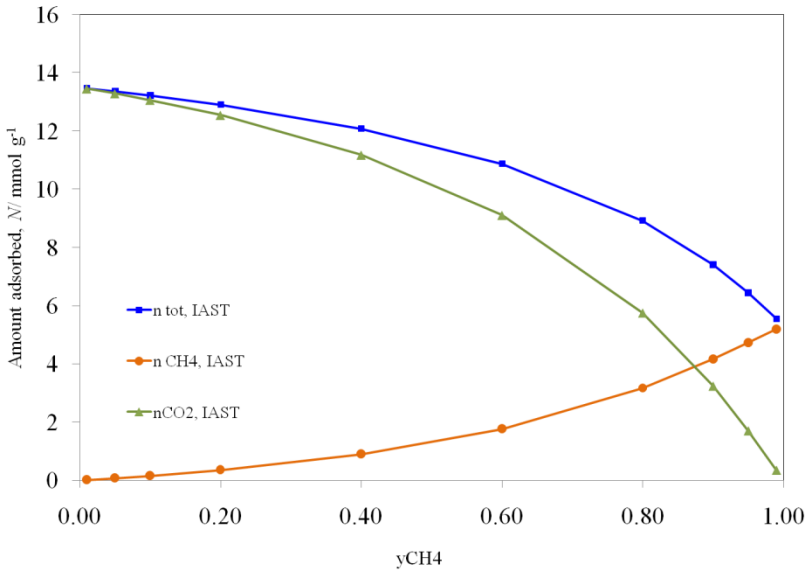

Figure 5.12: Variation of amount adsorbed from CO_2+CH_4 mixture at 305 K, P= 10 bar

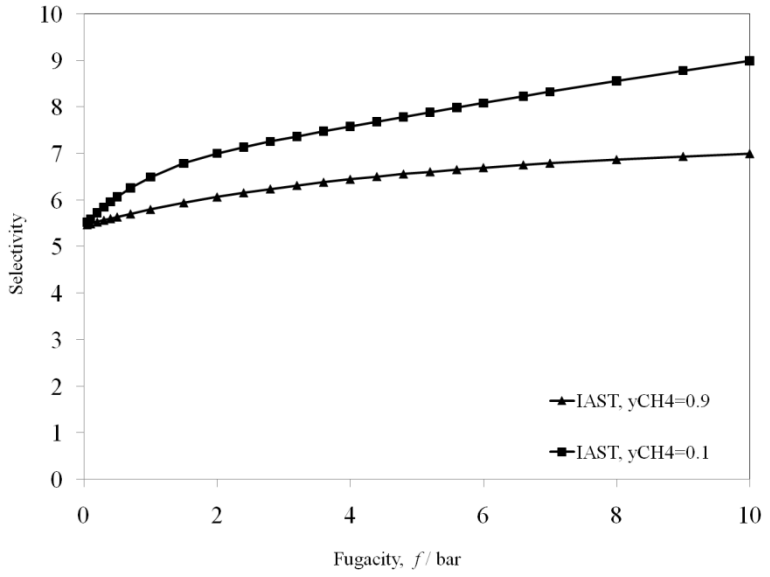

Figure 5.13: Variation of selectivity of CO_2+CH_4 mixture at 305 K with fugacity

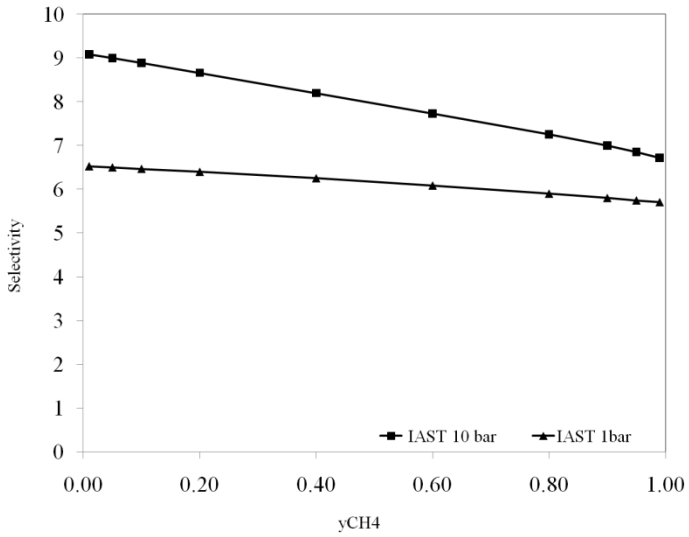

Figure 5.14: Variation of selectivity of CO_2+CH_4 mixture at 305 K with composition (in mole fraction)

In fact IAST was used in several works in literature earlier for estimation of binary adsorption properties of gas mixtures on this type of frameworks. The selectivity values predicted by IAST varied between 5.7 and 7.2. This selectivity for CO_2/CH_4 mixture thus shows promise for effective separation using Cu-BTC.

CHAPTER 6

CONCLUSIONS AND FUTURE WORKS

Literature Review of the experimental data on adsorption of CH_4 and CO_2 on various contemporary MOFs such as MIL-53(Al) and MIL-53(Cr), Cu-BTC, IRMOF-1 and IRMOF-3, MIL-101, as reported over the years by various researchers was done. The data was sorted and the best set of data was chosen base on the availability of data, the MOFs regenerability, heat of adsorption etc. It happened to be very difficult to do so as very few research work has been done where the pure gas adsorption for both the gases have been done on the MOF at the same lab. This was necessary to avoid any ambiguity arising out of the slight difference in surface properties appearing in MOFs formed at two different labs.

The pure gas sorption isotherm data so obtained was found for two MOFs Cu-BTC and Cr-BDC. The data was extracted and model fitted using Dual Site Langmuir and Virial Langmuir Isotherms which were found to be the most suitable. The corresponding Model Parameters were calculated. Cr-BDC was found to be showing two types of adsorption sites (metallic sites and Co-ordinatively Unsaturated Sites) and hence two saturation loadings.

Of the two Cu-BTC was found to be showing higher regeneration potential, more uniform pore size distribution in micropore (<2 nm) regime against Cr-BDC which due to its tendency to show higher degree of crystal imperfections during synthesis and is more prone towards rapid wear and tear when exposed to higher temperature and pressure in a packed bed adsorption column. Its due to these reasons that Cu-BTC was selected instead of Cr-BDC to next predict the mixed gas or binary behaviour of a mixture of the two gases by the Ideal Adsorbed Solution Theory which was done using the model parameters found earlier. The separation factor was calculated and plotted. It was found to vary in the range of 5.7 to 7.2. The separation factor thus is significant and this selectivity for CO_2/CH_4 mixture thus shows promise for effective separation using Cu-BTC in Pressure Swing Adsorption applications.

We leave this work after finding the separation factor and predicting the applicability of Cu-BTC adsorbent in PSA column design. Future scope may include actual designing of a PSA column in any process simulation software. The task could not be done ourself because of the fact that present day ASPEN plus software does not support Adsorption column design. Any work in future can be focussed on actual process design, provided such a software is available that supports adsorption column designs.

REFERENCES

[1] Yang, R. T., *Gas Separation by Adsorption Processes*, Imperial College Press, London (1997), Chapter-1.

[2] Ruthven, D. M. and Sun, M. S., *Principle of Adsorption and Adsorption Processes*, Wiley-Interscience, New York, (1984), Chapter-1.

[5] Yang, R. T., *Adsorbents: Fundamentals and Applications*, Wiley-Interscience, New-Jersey, (2003), p. 17-18

[7] Ruthven, D. M., Farooq, S. and Knaebel, *Pressure Swing Adsorption*, Wiley-VCH, New York, (1993), p. 12-13.

[8] Talu, O., "Needs, status, techniques and problems with binary gas adsorption experiments," *Adv. Coll. Inter. Sci.*, 76-77, 227-269 (1998).

[9] Yaghi, O. M., O'Keeffe, M., Ockwig, N. W., Chae, H. K., Eddaoudi, M., and Kim, J., "Reticular Synthesis and the design of New Materials," *Nature*, 423, 705-714 (2003).

[10] Rowsell, J. L. C., and Yaghi, O. M.," Metal–organic frameworks: a new class of porous materials," *Micropor. Mesopor. Mater.*, 73, 3-14 (2004).

[11] Panella, B., and Hirscher, M., "Hydrogen physisorption in metal– organic porous crystals," Adv. Mater. 17(5), 538–41 (2005).

[12] Panella, B., Hirscher, M., Putter, H., and Muller, U., "Hydrogen adsorption in metal–organic frameworks: Cu-MOFs and Zn-MOFs compared," AdvFunct Mater, 16(4), 520–4 (2006).

[13] Rowsell, J. L. C., Millward, A. R., Park, K. S., and Yaghi, O. M.," Hydrogen Sorption in Functionalized Metal-Organic Frameworks," J. Am. Chem. Soc., 126, 5666-5667 (2004).

[14] Wong-Foy, A. G., Matzger, A. J., and Yaghi, O. M., "Exceptional H_2 Saturation Uptake in Microporous Metal-Organic Frameworks," *J. Am. Chem. Soc.*, 128, 3494-3495 (2006).

[15] Pan, L., Sander, M. B., Huang, X., Li, J., Smith, M., Bittner, E., Bockrath, B., and Karl Johnson, J.," Microporous Metal Organic Materials: Promising Candidates as Sorbents for Hydrogen Storage," *J. Am. Chem. Soc.*, 126, 1308-1309 (2004).

[16] Férey, G., Latroche, M., Serre, C., Millange, F., Loiseau, T., and Percheron-Guégan, A., "Hydrogen adsorption in the nanoporous metal-benzenedicarboxylateM(OH)($O_2C–C_6H_4–CO_2$) (M = Al^{3+}, Cr^{3+}), MIL-53," *Chem. Commun.*, 2976-2977 (2003).

[17] Latroche, M., Surblé S., Serre, C., Mellot-Draznieks, C., Llewellyn, P. L., Lee, J. H, Chang, J. S., Jhung, S. H., and Férey, G., "Hydrogen Storage in the Giant-Pore Metal-Organic Frameworks MIL-100 and MIL-101," *Angew. Chem. Int. Ed.*, 45, 8227-8231 (2006).

[18] Li, Y., and Yang, R. T.,"Significantly Enhanced Hydrogen Storage in Metal-Organic Frameworks via Spillover," *J. Am. Chem. Soc.*, 128, 726-727 (2006).

[19] Van de Voorde, M., Verelst, H., and Baron, G.V., "Measurement of O_2-N_2 Binary Sorption on 5A Zeolite by Isotope Tracer and Perturbation Chromatography," *J. Porous Materials*, 2, 51-57 (1995).

[20] Staudt, R., Herbst, A., Beutekamp S., and Harting, P., "Adsorption of Pure Gases and Mixtures on Porous Solids up to High Pressures," *Adsorption*, 11, 379-384 (2005).

[21] Shen, D., and Bülow, M., "Comparison of Experimental Techniques for Measuring Isosteric Heat of Adsorption," *Adsorption*, 6, 275-286 (2000).

[22] Talu, O., and Zwiebel, I., "Multicomponent Adsorption Equilibria of Nonideal Mixtures", *AIChE J.*,32, 1263-1276 (1986).

[23] Li, Y., and Yang, R.T., "Gas Adsorption and storage in Metal-Organic Framework MOF-177," *Langmuir*, 23, 12937-12944 (2007).

[24] D. K. Friday and M. D. LeVan, "Hot Purge Gas Regeneration of Adsorption Beds Solute Condensation: Experimental Studies,"AIChE J., 31, 1322 (1985).

[25] Mueller, U., Schubert, M., Teich, F., Puetter, H., Schierle-Arndt, K., and Pastré, J.,"Metal-organic Frameworks-Prospective Industrial Applications," *J. Mater. Chem.*, 16, 626-636 (2006).

[26] Keller, J. U., Saudt, R., "Gas Adsorption equilibria experimental methods and Adsorptive Isotherms" Springer Sci. Inc., 2005, Chapter 1, 7.

[27] Eddaoudi, M., Moler, D. B., Li, H., Chen, B., Reineke, T. M., O'Keeffe, M., and Yaghi, O. M.,"Modular Chemistry: Secondary Building Units as a Basis for the design of Highly Porous Metal-Organic Carboxylate Frameworks," *Acc. Chem. Res.*, 34, 319-330 (2001).

[28] Sarkisov, L., Düren, T., and Snurr, R.Q., "Molecular modeling of adsorption in novel nanoporous metal-organic materials," *Mol. Phys.*, 102, 211-221 (2004)

[29] Do, D. D., *Adsorption Analysis: Equilibria and Kinetics*, Imperial College Press, London, 1998.

[30] Düren, T., and Snurr, R.Q., "Assessment of Isoreticular Metal-Organic Frameworks for Adsorption Separations: A Molecular Simulation Study of Methane/*n*-Butane Mixtures," *J. Phys. Chem. B*, 108, 15703-15708 (2004).

[31] Baker, R.W., and Lokhandwala, K., "Natural gas processing with membranes: An overview," Ind. Eng. Chem. Res., vol. 47(7), pp. 2109-2121, 2008.

[32] Eddaoudi, M., Li, H., and Yaghi, O. M.," Highly Porous and Stable Metal-Organic Frameworks: Structure, Design and Sorption Properties," *J. Am. Chem. Soc.*, 122, 1391-1397 (2000).

[33] Huang, L., Wang, H., Chen, J., Wang, Z., Sun, J., Zhao, D., and Yan, Y.,"Synthesis, Morphology Control, and Properties of Porous Metal-Organic Coordination Polymers," *Micropor. Mesopor. Mater.*, 58, 105-114 (2003).

[34] Liu, B., and Smit, B.,"Comparative Molecular Simulation Study of CO_2/N_2 and CH_4/N_2 Separation in Zeolites and Metal-Organic Frameworks," *Langmuir*, 25, 5918-5926 (2009).

[35] Keskin, S., and Sholl, D. S.," Screening Metal-Organic Framework Materials for Membrane-based Methane/Carbon Dioxide Separations," *J. Phys. Chem. C*, 111, 14055-14059 (2007).

[36] Liang, Z., Marshall, M., and Chaffee, A.L., "CO_2 Adsorption-Based Separation by Metal Organic framework (Cu-BTC) versus Zeolite (13X)," *Energy & Fuels*, 23, 2785-2789 (2009)

[37] Vishnyakov, A., Ravikovitch, P. I., Neimark, A. V., Bülow, M., Wang, Q. M.,"Nanopore structure and sorption properties of Cu-BTC metal-organic framework," *Nano Lett.*, 3, 713-718 (2003).

[38] Wang, Q.M., Shen, D., Bülow, M., Lau, M. L., Deng, S., Fitch, F. R., Lemcoff, N. O., Semanscin, J.,"Metallo-organic molecular sieve for gas separation and purification," *Micropor. Mesopor. Mater.*, 55, 217-230 (2002).

[39] Wang, S., Yang, Q., and Zhong, C.,"Adsorption and separation of binary mixtures in a metal-organic framework Cu-BTC: A computational study," *Sep. Purf. Tech.*, 60, 30-35 (2008).

[40] Yang, Q., Xue, C., Zhong, C., and Chen, J. –F.,"Molecular Simulation of Separation of CO_2 from Flue Gases in Cu-BTC Metal-Organic Framework," *AIChE J.*, 53, 2832-2840 (2007).

[41] Eddaoudi, M., Kim, J., Rosi, N., Vodak, D., Wachter, J., O'Keeffe, M., Yaghi, O. M.," Systematic Design of Pore Size and Functionality in Isoreticular MOFs and Their Application in Methane Storage," *Science*, 295, 469-472 (2002).

[42] Bourrelly, S., Llewellyn, P. L., Serre, C., Millange, F., Loiseau, T., and Férey, G., "Different Adsorption Behaviors of Methane and Carbon Dioxide in the Isotypic Nanoporous Metal Terephthalates MIL-53 and MIL-47," *J. Am. Chem. Soc.*, 127, 13519-13521 (2005).

[43] Millward, A. R., and Yaghi, O. M.," Metal-Organic Frameworks with Exceptionally High Capacity for Storage of Carbon Dioxide at Room Temperature," *J. Am. Chem. Soc.*, 127, 17998-17999 (2005).

[44] Senkovska, I. and Kaskel, S.," High pressure methane adsorption in the metal-organic frameworks $Cu_3(btc)_2$, $Zn_2(bdc)_2dabco$, and $Cr_3F(H_2O)_2O(bdc)_3$," *Micropor. Mesopor. Mater.*, 112, 108-115 (2008).

[45] Llewellyn, P.L., Bourrelly, S., Serre, C., Vimont, A., Daturi, M., Hamon, L., Weireld, G. D., Chang, J. -S., Hong, D. -Y., Hwang, Y. K., Jhung, S. H., Férey, G., "High Uptakes of CO_2 and

CH_4 in Mesoporous Metal-Organic Frameworks MIL-100 and MIL-101," *Langmuir*, 24, 7245-7250 (2008).

[46] S. Bureekaew, S. Shimomura, S. Kitagawa, Sci. Technol. Adv. Mater. 9 (2008) 014108.

[47] Jarvis, J.A.J., Acta Crystallographica 15 (1962) 964–966.

[48] Okada, K., Kay, M.I., Cromer, D.T., Almodovar, I., "Crystal Structure by Neutron Diffraction and the Antiferroelectric Phase Transition in Copper Formate Tetrahydrate," J. Chem. Phys. 44,1648-1653 (1966)

[49] Sterling, C., Science 146 (1964) 518–519.

[50] Chui, S. S.-Y., Lo, S. M.-F., Charmant, J. P. H., Orpen, A. G., and Williams, I. D.,"A Chemically Functionalizable Nanoporous material $[Cu_3(TMA)_2(H_2O)_3]_n$," *Science*, 283, 1148-1150 (1999).

[51] Rowsell, J. L. C., and Yaghi, O. M., "Effects of Functionalization, Catenation, and Variation of the Metal Oxide and Organic Linking Units on the Low-Pressure Hydrogen Adsorption Properties of Metal-Organic Frameworks," J. Am. Chem. Soc., 128, 1304-1315 (2006).

[52] Férey, G., Mellot-Draznieks, C., Serre, C., Millange, F., Dutour, J., Surblé S., and Margiolaki, I., "A Chromium Terephthalate-Based Solid with Unusually Large Pore Volumes and Surface Area," Science, 309, 2040-2042 (2005).

[53] Cavenati, S., Grande, C.A., Rodrigues, A.E., Energy Fuels 20 (2006) 2648.

[54] Delgado, J.A., Uguina, M.A., Sotelo, J.L., Ruiz, B., Gómez, J.M.: Fixed-bed adsorption of carbon dioxide/methane mixtures on silicalite pellets. Adsorption 12, 5–18 (2006a) [55] S. Cavenati, C.A. Grande, A.E. Rodrigues, Ind. Eng. Chem. Res. 47 (2008) 6333

[56] Gomes, V.G., Hassan, M.M., Coalseam methane recovery by vacuum swing adsorption, Sep. Purif. Technol. 24 (2001) 189

[57] Schlichte, K., Kratzke, T., and Kaskel, S.,"Improved synthesis, thermal stability and catalytic properties of the metal-organic framework compound $Cu_3(BTC)_2$," *Micropor. Mesopor. Mater.*, 73, 81-88 (2004).

[58] Delgado, J.A., Uguina, M.A., Sotelo, J.L., Ruiz, B., "Fixed-bed adsorption of carbon dioxide/methane mixtures on silicalite pellets", Adsorption, 12,5-18, (2006).

[59] Rochelle, G. T., "Amine scrubbing for CO_2 capture," Science 325(5948), 1652–1654. (2009).

[60] Yang, R.T. , Gas Separation by Adsorption Processes, World Scientific, Singapore,1997.

[61] Chui, SSY · Lo, SMF · Charmant, JPH · Orpen, AG · Williams, ID. 1999. Science. v. 283, (5405), 1999, FEB 19, p. 1148-1150 [62] H. Li, M. Eddaoudi, M. O'Keeffe, O.M. Yaghi, Nature 402 (1999) 276–279.

[63] Prestipino, C., Regli, L., Vitillo, J. G., Bonino, F., Damin, A., Lamberti, C., Zecchina, A., Solari, P. L., Kongshaug, K. O., and Bordiga, S., "Local Structure of Framework Cu(II) in HKUST-1 Metallorganic Framework: Spectroscopic Characterization upon Activation and Interaction with Adsorbates," *Chem. Mater.*, 18, 1337-1346 (2006).

[64] Szeto, K. C., Lillerud, K. P., Tilset, M., Bjørgen, M., Prestipino, C., Zecchina, A., Lamberti, C., and Bordiga, S., "A Thermally Stable Pt/Y-Based Metal-Organic Framework: Exploring the Accessibility of the Metal Centers with Spectroscopic Methods Using H_2O, CH_3OH, and CH_3CN as Probes," *J. Phys. Chem. B*, 110, 21509-21520 (2006).

[65] Alaerts, L., Séguin, E., Poelman, H., Thibault-Starzyk, F., Jacobs, P.A., and De Vos, D.E., "Probing the Lewis Acidity and Catalytic Activity of the Metal-Organic Framework $[Cu_3(btc)_2]$ (BTC=Benzene-1,3,5-tricarboxylate)," *Chem. Eur. J.*, 12, 7353-7363 (2006).

[66] Klein, N., Senkovska, I., Gedrich, K., Stoeck, U., Henschel, A., Mueller, U., Kaskel, S., Angew. Chem. Int. Ed. 48 (2009) 9954–9957.

[67] Hartmann, M., Kunz, S., Himsl, D., Tangermann, O., Ernst, S., Wagener, A., Langmuir 24 (2008) 8634–8642.

[68] Tranchemontagne, D.J., Mendoza-Cortés, J.L., O'Keeffe, M., Yaghi, O., Chem. Soc. Rev. 38 (2009) 1257–1283.

[69] Farrusseng, D., Daniel, C., Gaudillere, C., Ravon, U., Schuurman, Y., Mirodatos, C., Dubbeldam, D., Frost, H., and Snurr, R.Q., "Heats of Adsorption for Seven Gases in Three Metal-Organic Frameworks: Systematic Comparison of Experiment and Simulation," *Langmuir*, 25, 7383-7388 (2009).

[70] Rao, C. N. R., Natarajan, S., and Vaidhyanathan, R.,"Metal Carboxylates with Open Architectures, " *Angew. Chem. Int. Ed.*, 43, 1466-1496 (2004).

[71] García-Pérez, E., Gascón, J., Morales-Flórez, V., Castillo, J.M., Kapteijn, F., and Calero, S., "Identification of Adsorption sites in Cu-BTC by Experimentation and Molecular Simulation," *Langmuir*, 25, 1725-1731 (2009).

[72] Yazaydin, A.O., Snurr, R.Q., Park, T.-H., Koh, K., Liu, J., LeVan, M.D., Benin, A.I., Jakubczak, P., Lanuza, M., Galloway, D.B., Low, J.J., and Willis, R.R., "Screening of Metal-Organic Frameworks for Carbon Dioxide Capture from Flue Gas Using a Combined Experimental and Modeling Approach," *J. Am. Chem. Soc.*, 131, 18198-18199 (2009).

[73] Zhao, Z., Li, Z., and Lin, Y.S., "Adsorption and Diffusion of Carbon Dioxide on Metal-Organic Framework (MOF-5)," *Ind. Eng. Chem. Res.*, 48, 10015-10020 (2009).

[74] Férey, G., Mellot-Draznieks, C., Serre, C., Millange, F., Dutour, J., Surblé S., and Margiolaki, I., "A Chromium Terephthalate-Based Solid with Unusually Large Pore Volumes and Surface Area," *Science*, 309, 2040-2042 (2005).

[75] Lebedev, O. I., Millange, F., Serre, C., Van Tendeloo, G., and Férey, G.," First Direct Imaging of Giant Pores of the Metal-Organic Framework MIL-101," *Chem. Mater.*, 17, 6525-6527 (2005).

[76] Garberoglio, G., Skoulidas, A.I., and Karl Johnson, J., "Adsorption of Gases in Metal Organic Materials: Comparison of Simulations and Experiments," *J. Phys. Chem. B*, 109, 13094-13103 (2005).

[77] Salem, M.M.K., Braeuer, P., Szombathely, M.V., Heuchel, M., Harting, P., Quitzsch, K., and Jaroniec, M., "Thermodynamics of High-Pressure Adsorption of Argon, Nitrogen, and Methane on Microporous adsorbents," *Langmuir*, 14, 3376-3389 (1998).

[78] Wang, S., "Comparative Molecular Simulation Study of Methane adsorption in Metal-Organic frameworks," *Energy & Fuels*, 21, 953-956 (2007).

[79] Liu, J., Culp, J.T., Natesakhawat, S., Bockrath, B.C., Zande, B., Sankar, S.G., Garberoglio, G., and Karl Johnson, J., "Experimental and Theoretical Studies of Gas Adsorption in $Cu_3(BTC)_2$: An Effective Activation Procedure," *J. Phys. Chem. C.*, 111, 9305-9313 (2007).

[80] Finsy, V., Ma, L., Alaerts, L., De Vos, D.E., Baron, G.V., Denayer, J. F. M., "Separation of CO_2/CH_4 mixtures with the MIL-53(Al) metal–organic framework," *Micropor. Mesopor. Mater.*, 120, 221-227 (2009).

[81] Karra, J. R., and Walton, K. S.," Effect of Open Metal Sites on Adsorption of Polar and Nonpolar Molecules in Metal-Organic Framework Cu-BTC, " *Langmuir*, 24, 8620-8626 (2008).

[82] Myers, A.L., "Characterization of nanopores by standard enthalpy and entropy of adsorption of probe molecules," Colloids and Surfaces A, 241, 9-14 (2004).

[83] Sircar, S., "Role of adsorbent heterogeneity on mixed gas adsorption," *Ind. Eng. Chem. Res.*, 30, 1032-1039 (1991).

[84] Chowdhury P., Jedidiah S., Dreisbach F., and Gumma S., "Adsorption of CO, CO_2 and CH_4 on Cu-BTC and MIL-101 Metal Organic Frameworks: Effect of Open Metal Sites and Adsorbate Polarity," Microporous and Mesoporous Materials, 152, 246-252, 2012.

[85] Chowdhury, P., Bikkina, C., and Gumma, S.,"Gas Adsorption Properties of the Chromium-Based Metal Organic Framework MIL-101, " *J. Phys. Chem. C*, 113, 6616-6621 (2009).

[86] Heslop, M.J., Buffham, B.A., and Mason,G., "A Test of the Polynomial-Fitting Method of Determining Binary-Gas-Mixture Adsorption Equilibria", *Ind. Eng. Chem. Res.*, 35, 1456-1466 (1996).

[87] Smith, J. M. and Van Ness H. C., *Introduction to Chemical Engineering Thermodynamics*, Fourth Edition, McGraw-Hill, New York, (1987).

[88] Myers, A. L., and Prausnitz, J. M., "Thermodynamics of Mixed Gas Adsorption," *AIChE J.*, 11,121-127 (1965).

[89] Talu, O., *Thermodynamics of multicomponent gas adsorption equilibria of non-ideal mixtures*, PhD Dissertation, Arizona State University (1984).

[90] Hoory, S. E., and Prausnitz, J. M., "Monolayer adsorption of gas mixtures on homogeneous and heterogeneous solids", *Chem. Eng. Sci.*, 22, 1025-1033 (1967).

[91] Siperstein, F.R., and Myers, A.L., "Mixed-Gas Adsorption," *AIChE J.*, 47, 1141-1159 (2001).

[92] Van Ness, H. C., "Adsorption of gases on solids," *I & EC Fundamentals*, 8, 464-473 (1969).

[93] Steele, W. A., *The interaction of gases with solid surfaces*, Pergamon press, New York,

[94] Mathias, P. M., Kumar, R., Moyer, J. D., Schork, J. J. M., Srinivasan, S. R., Auvil, S. R., and Talu, O., "Correlation of Multicomponent Gas Adsorption by the Dual-Site Langmuir Model. Application to Nitrogen/Oxygen Adsorption on 5A-Zeolite," *Ind. Eng. Chem. Res.*, 35, 2477-2483 (1996).

[95] Ross, S., and Olivier, J. P., *On physical adsorption*, Buttersworth, Washington D.C., (1964).

[96] Ustinov, E. A., Do, D. D., Herbst, A., Staudt, R., and Harting, P., "Modeling of Gas Adsorption equilibrium over a Wide Range of pressure: A Thermodynamic Approach Based on Equation of State," *J. Coll. Inter. Sci.*, 250, 49-62 (2002).

[97] Taqvi, S.M., and LeVan, D.M., "Virial Description of Two-Component Adsorption on Homogeneous and Heterogeneous Surfaces", *Ind. Eng. Chem. Res.*, 36, 2197-2206 (1997).

[98] Appel, W.S., LeVan, D.M., and Finn, J.E., "Nonideal Adsorption Equilibria Described by Pure Component Isotherms and Virial Mixture Coeffcients", *Ind. Eng. Chem. Res.*, 37, 4774-4782 (1998).

[99] Yaghi, O. M., Li, G., and Li, H., "Selective binding and removal of guests in a microporous metal-organic framework," *Nature*, 378, 703-706 (1995).

[100] Green, D.W. Perry R. H., Perry's Chemical Engineers' Handbook,8th Edition, The McGraw-Hill Companies, Inc. Chapter 16, pg 52-55.